ANALYSIS OF RETREAT MINING PILLAR STABILITY (ARMPS)

By Christopher Mark, Ph.D.,[1] and Frank E. Chase[2]

ABSTRACT

The prevention of pillar squeezes, massive pillar collapses, and bumps is critical to safe pillar recovery operations. To help prevent these underground safety problems, the Pittsburgh Research Center has developed the Analysis of Retreat Mining Pillar Stability (ARMPS) computer program. ARMPS calculates stability factors (SF) based on estimates of the loads applied to, and the load-bearing capacities of, pillars during retreat mining. The program can model the significant features of most retreat mining layouts, including angled crosscuts, varied spacings between entries, barrier pillars between the active section and old (side) gobs, and slab cuts in the barriers on retreat. It also features a pillar strength formula that considers the greater strength of rectangular pillars. The program may be used to evaluate bleeder designs, as well as active workings.

A data base of 140 pillar retreat case histories has been collected across the United States to verify the program. It was found that satisfactory conditions were very rare when the ARMPS SF was less than 0.75. Conversely, very few unsatisfactory designs were found where the ARMPS SF was greater than 1.5. Preliminary analyses also indicate that pillar failures are more likely beneath sandstone roof and that the ARMPS SF may be less meaningful when the depth of cover exceeds 230 m (750 ft).

[1]Mining engineer.
[2]Geologist.
Pittsburgh Research Center, National Institute for Occupational Safety and Health, Pittsburgh, PA.

INTRODUCTION

The use of remote-control continuous miners, extended cuts, and mobile roof supports has increased the productivity of room-and-pillar retreat mining (also referred to as "pillaring," "pillar recovery," "robbing," and "second mining"). In the southern Appalachian coalfields, many mines are choosing room-and-pillar retreat mining because of its lower capital cost and greater flexibility [Blaiklock 1992]. Unfortunately, between 1989 and 1996, 25% of all roof and rib fatalities occurred on pillar recovery sections.

Roof fall accidents are not the only problem associated with retreat mining. Millions of tons of coal are sterilized annually because of pillar squeezes, floor heave, pillar line roof falls, and pillar bumps. Traditional pillar design methods are of little help due to the complex mining geometries and abutment pressures that are present during pillar extraction. The Pittsburgh Research Center has developed the Analysis of Retreat Mining Pillar Stability (ARMPS) computer program to aid in the design of pillar recovery operations. This paper describes the program and presents the findings thus far.

THE ARMPS METHOD

The goal of ARMPS is to help ensure that the pillars developed for future extraction (production pillars) are of adequate size for all anticipated loading conditions. The key is to be able to estimate the magnitudes of the various loads that the pillars might experience throughout the mining process. The formulas used in ARMPS are based on those originally developed for the Analysis of Longwall Pillar Stability (ALPS) method, which is widely used for longwall pillar design [Mark 1990, 1992]. ALPS was initially derived from underground measurements of longwall abutment stresses and was later validated by the back-analysis of more than 100 case histories.

In ARMPS, the formulas have been extensively modified for the variety of mining geometries typically found in pillar recovery operations.

USER INPUT

The first step in using the ARMPS program is to enter the dimensions of the pillars in the working section, as illustrated in figure 1. The program can accommodate angled crosscuts, varied spacings between the entries, and barrier pillars between the active section and old (side) gob areas. Slabbing of barriers
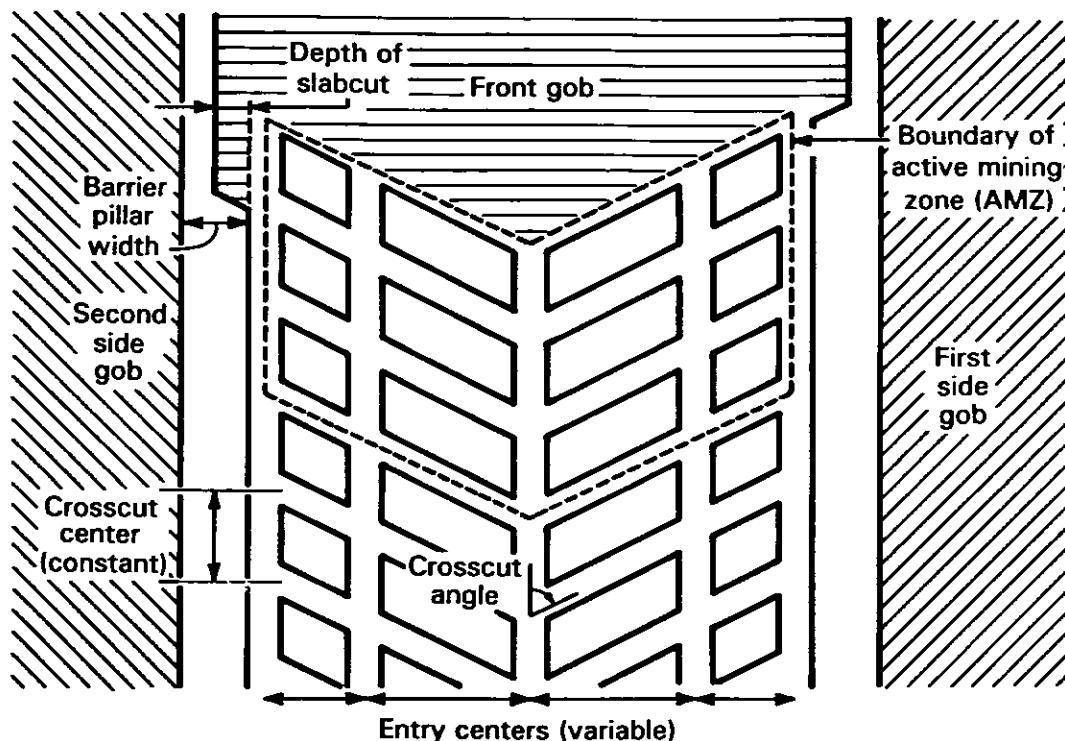

Figure 1.—Section layout parameters used in ARMPS.

on retreat can also be included. Other parameters that must be defined include depth of cover, mining height, entry width, and crosscut spacing. Finally, the user chooses one of four possible *loading conditions* (figure 2). The simplest, loading Condition 1, is development loading only. Loading condition 2 occurs when the active, or "front," panel is being fully retreated and there are no adjacent mined-out areas. The total applied load is the sum of the development loads and the front abutment load. Loading condition 3 occurs where the active mining zone (AMZ) is adjacent to an old (side) gob and the pillars are subjected to development, side abutment, and front abutment loads. Where the pillar line is surrounded by gob on three sides (sometimes referred to as "bottlenecking"), loading condition 4 is used. In every case, the extent of each gob is defined by the user.

ARMPS STABILITY FACTOR FOR THE ACTIVE MINING ZONE

The basic output from the ARMPS program is the stability factor (SF), defined as

$$ARMPS\ SF = LBC/LT, \tag{1}$$

where LBC = the estimated total load-bearing capacity of the pillars within the AMZ,

and LT = the estimated total load applied to pillars within the AMZ.

Figure 3 illustrates the development and front abutment loads applied to the AMZ.
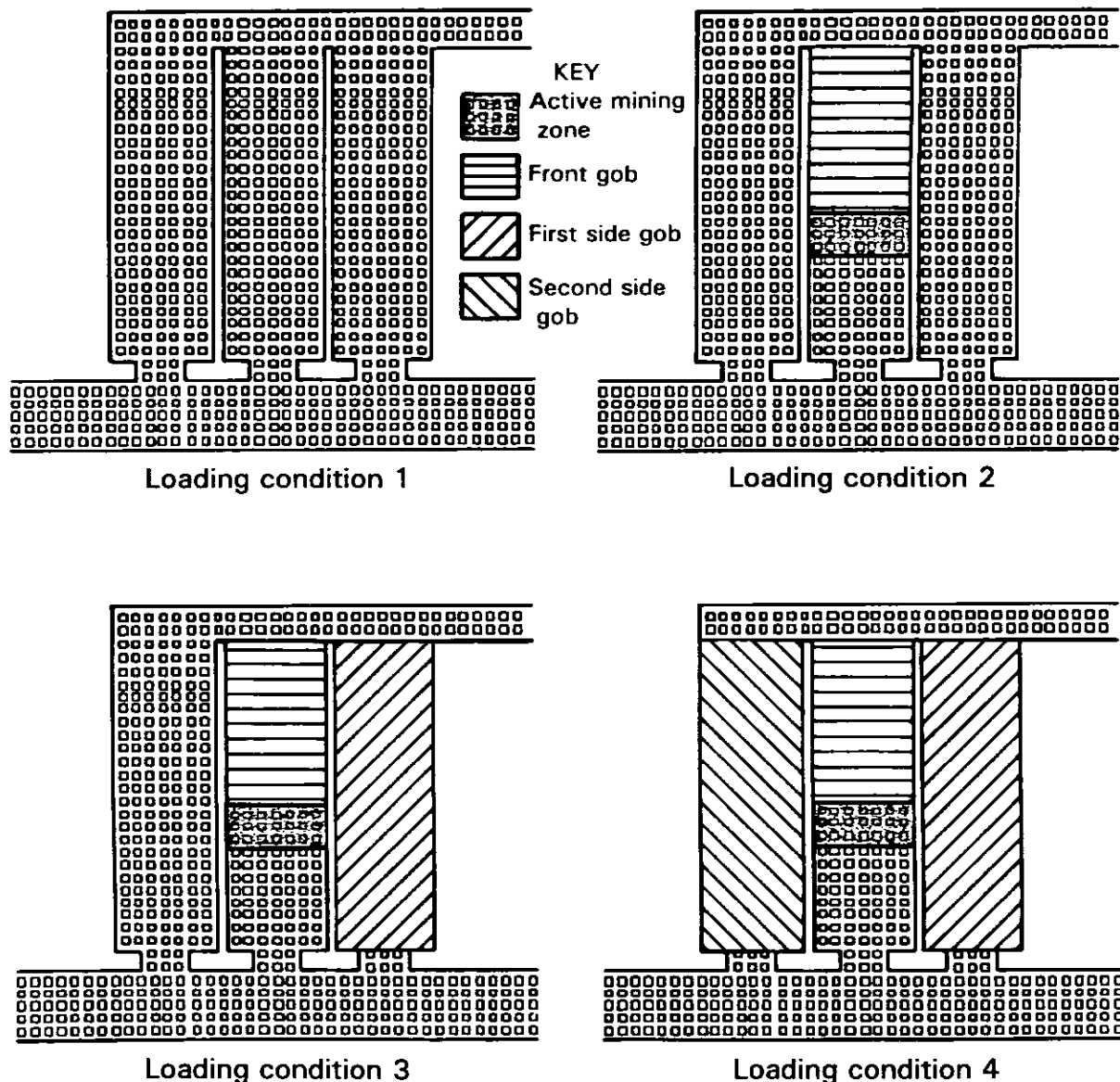

KEY

Active mining zone

Front gob

First side gob

Second side gob

Loading condition 1

Loading condition 2

Loading condition 3

Loading condition 4

Figure 2.—The four loading conditions that can be evaluated with ARMPS.

KEY

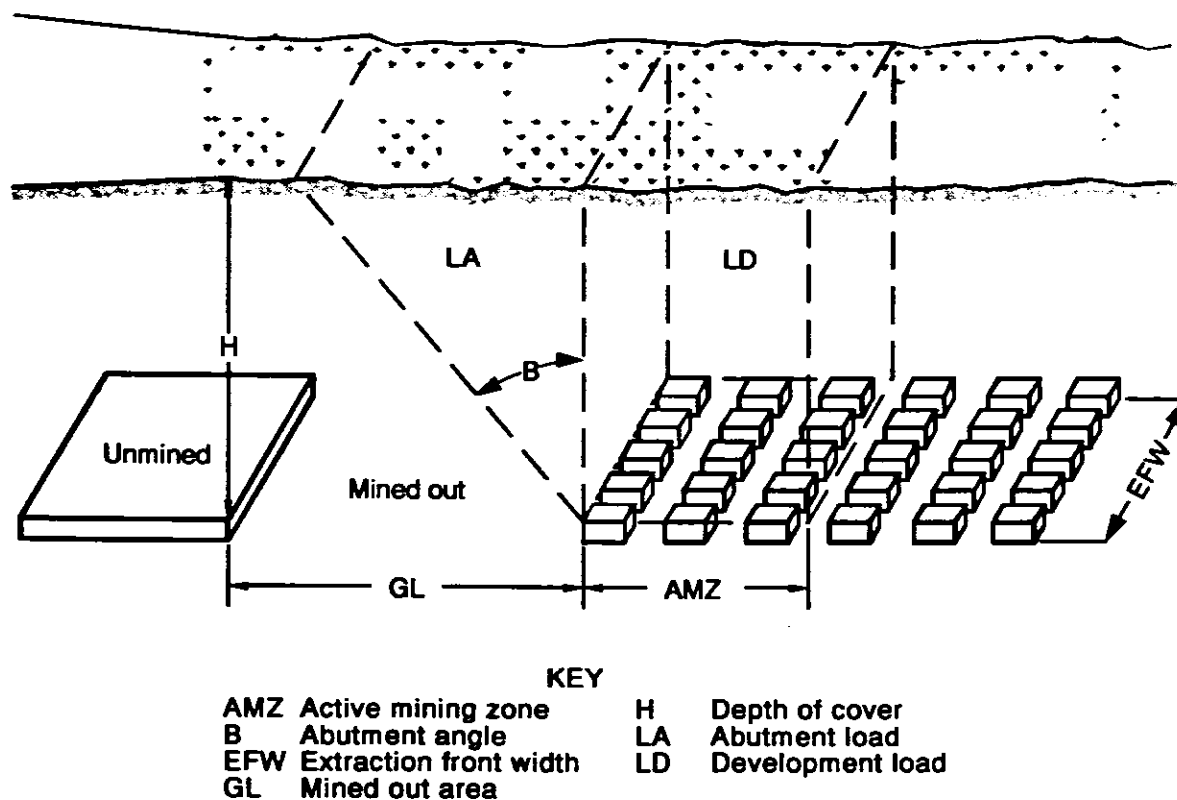|			
AMZ	Active mining zone	H	Depth of cover
B	Abutment angle	LA	Abutment load
EFW	Extraction front width	LD	Development load
GL	Mined out area		

Figure 3.—Schematic showing the active mining zone, the development load, and the front abutment load.

The AMZ includes all of the pillars on the extraction front (or "pillar line") and extends outby the pillar line a distance of five times the square root of the depth of cover ($5\sqrt{H}$). This distance was selected because measurements of abutment stress distributions [Mark 1990] show that 90% of the front abutment load falls within its boundaries (figure 4).

ARMPS calculates the SF for the entire AMZ, rather than stability factors for individual pillars, because experience has shown that the pillars within the AMZ typically behave as a *system*. If an individual pillar is overloaded, it will normally transfer its excess load to adjacent pillars. If those pillars are adequately sized, the process ends there. A pillar squeeze occurs only when the adjacent pillars are also undersized. They then fail in turn, resulting in a "domino" of load transfer and pillar failure. The ARMPS SF is therefore a measure of the overall stability of the pillar system.

PILLAR LOAD-BEARING CAPACITY

The load-bearing capacity of the AMZ is calculated by summing the load-bearing capacities of all of the pillars within its boundaries. The strength of an individual pillar (SP) is determined using a new pillar strength formula (the Mark-Bieniawski formula) that considers the effect of pillar length:

$$SP = S_1 [0.64 + (0.54 - 0.18 (w^2/hL))], \qquad (2)$$

where S_1 = in situ coal strength, assumed = 6.2 MPa (900 psi),

w = pillar width,

h = pillar height,

and L = pillar length.

The new pillar strength formula was needed because the pillars used in retreat mining are often much longer than they are wide. The strength of rectangular pillars can be significantly greater than square pillars due to the greater confinement generated within them. The Mark-Bieniawski formula was derived from analyses of the pillar stress distributions implied by empirical pillar strength formulas. A complete discussion of the Mark-Bieniawski formula is included in appendix A of this paper. The in situ coal strength is assumed to be 6.2 MPa (900 psi) in ARMPS; however, this value can be modified by the user.

The load-bearing capacity of the pillars is determined by multiplying their strength by their load-bearing area. When angled crosscuts are employed, the algorithm still calculates accurately each pillar's least dimension, length, and load-bearing area (A_p):
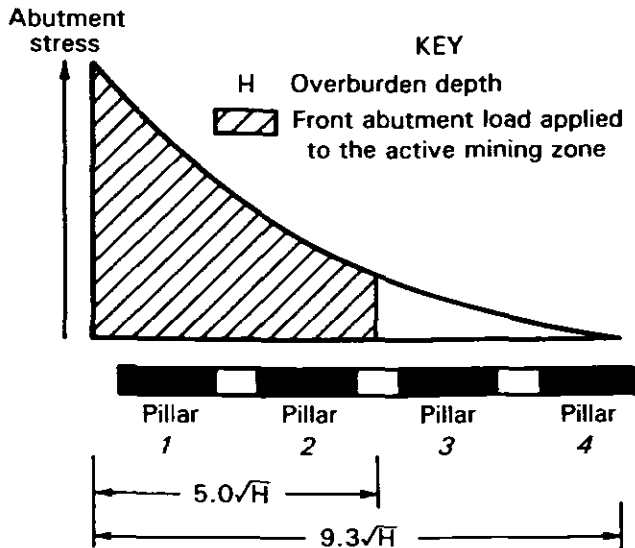
KEY

H   Overburden depth

  Front abutment load applied to the active mining zone

Figure 4.—Distribution of abutment stress, showing that 90% of the abutment falls within the distance of (5√H) from the gob edge.

$$A_p = [(XC)(ECTR) - (XC)(W_e) - (ECTR)(W_e)/(sin \phi)$$
$$+ (W_e)^2/(sin \phi)], \tag{3}$$

where   XC   = center-to-center crosscut spacing,

           ECTR   = center-to-center entry spacing,

           W_e = entry width,

and ϕ = angle between the crosscut and the entry.

The load-bearing capacity of the pillar system is then obtained by summing the capacities of the individual pillars within the AMZ. ARMPS calculates the strength and load-bearing capacity of barrier pillars in the same manner as the panel pillars, except that their length is limited to the breadth of the AMZ.

PILLAR LOADINGS

The loadings applied to the AMZ include development loads, abutment loads, and loads transferred from barrier pillars. Table 1 shows the sources of loads and the loading conditions in which they occur.

Table 1.—Loads applied to the active mining zone in ARMPS

Source of load	Loading condition			
	1	2	3	4
Development	X	X	X	X
Front abutment		X	X	X
Side gob abutments			X	X
Transfer from barriers between active mining zone and side gobs			X	X
Transfer from remnant barriers between front gob and side gobs			X	X

Development loads are due to the weight of the overburden directly above the pillars before any retreat mining takes place. The tributary area theory is used in ARMPS to estimate development loads.

Abutment loads occur as a result of retreat mining and gob formation. They are determined by the depth of cover, the extent of the gobs, the width of the extraction front, and the abutment angles. These parameters are illustrated in two dimensions in figure 5. The abutment angle determines how much load is carried by gob. Measurements of longwall abutment stresses indicated that an abutment angle of 21° is appropriate for normal caving conditions [Mark 1992]. The ARMPS program initializes the abutment angles for all gobs to 21°; however, this can be changed by the user. For example, if it is known that no caving has occurred, then the abutment angle may be set to 90° to simulate zero load transfer to the gob [Chase and Mark 1993].

The abutment stresses are assumed to be distributed following the inverse-square function shown in figure 4. Abutment loads are also applied to barrier pillars; however, if a barrier is too small to carry its share, then some or all of the excess is transferred to the AMZ.

The front abutment load applied to the AMZ is calculated as follows. The volume of the overburden above the mined-out active gob is the depth of cover multiplied by the gob area. The portion of this volume whose weight is carried by the gob is determined by the tangent of the abutment angle, as shown in figure 5. This portion is subtracted, and the remainder is shared between the AMZ and the unmined coal on the other three sides of the gob. It is assumed that barrier pillars (or substantial production pillars) are present on the other three sides of the gob. Load applied to the barriers here may be transferred back to the AMZ if the barriers are removed later in the mining process.

The magnitude of the front abutment load applied to the AMZ is determined by the extent of the extraction zone and the depth of cover. The front abutment is considered fully developed if the gob area is large relative to the depth of cover (figure 6A). If only a few rows of pillars have been extracted (figure 6B), much of the load will be carried by the back barrier. If the full extraction zone is rather narrow (figure 6C), much of the load will be carried by the side barriers.
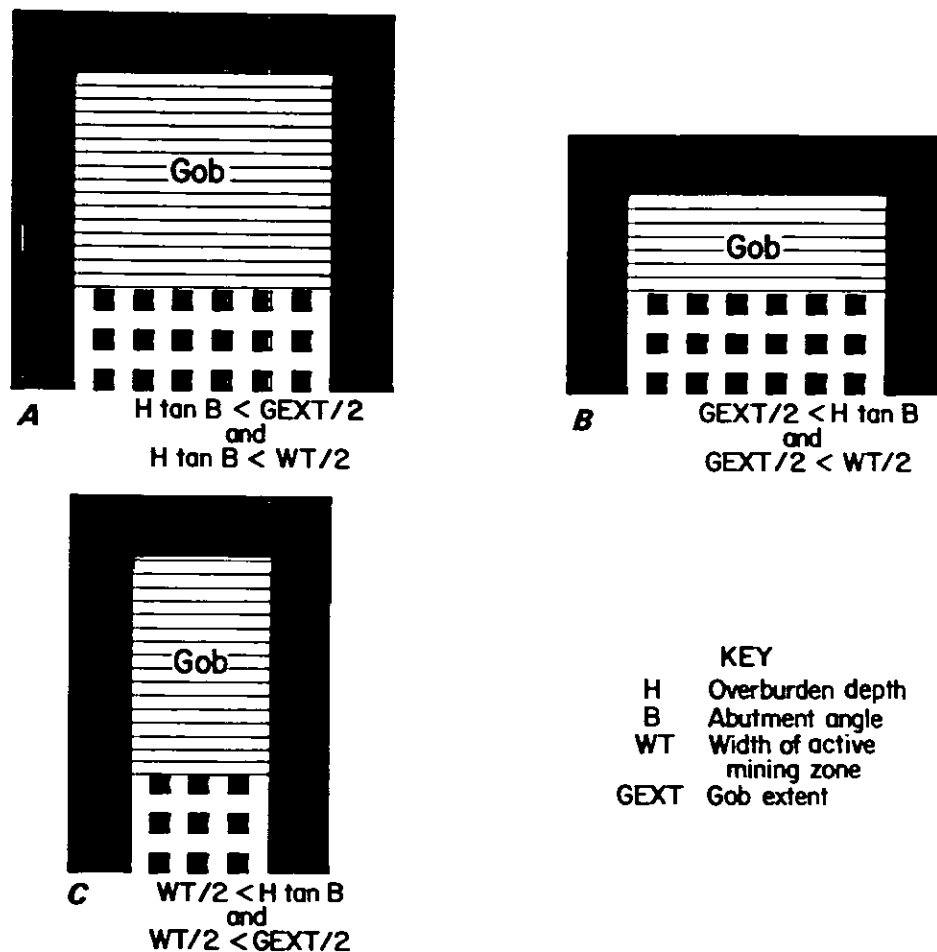
The side abutment loads are shared by the AMZ and, if it is present, the barrier pillar between the AMZ and the side gob. The inverse-square stress distribution (figure 4) again is used to apportion the load between the barrier and the AMZ. Next, if it is determined that the barriers are overloaded, some additional side abutment load is transferred to the AMZ.

To determine whether a barrier pillar can carry the load applied to it, ARMPS estimates the barrier's SF by dividing its load-bearing capacity by its load. The total load applied to a barrier pillar is the sum of the development load, the front abutment load due to any slabbing, and the side abutment load applied to the barrier. If the SF is greater than 1.5, the barrier is assumed to be stable. When the barrier's SF is between 1.5

A ... LS ... LDEV ... H ... B ... H tan B ... DEPAMZ

B ... LS ... LDEV ... H ... B ... GEXT/2 ... DEPAMZ
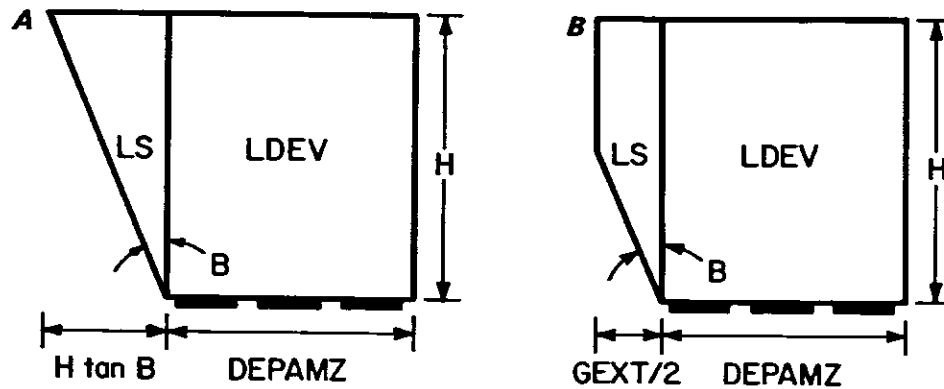
KEY

H	Overburden	GEXT	Gob extent
LS	Abutment load	DEPAMZ	Breadth of active
LDEV	Development load		mining zone
B	Abutment angle		

Figure 5.—Schematic showing the abutment load in two dimensions. A, supercritical gob; B, subcritical gob.

A
H tan B < GEXT/2
and
H tan B < WT/2

B
GEXT/2 < H tan B
and
GEXT/2 < WT/2

C
WT/2 < H tan B
and
WT/2 < GEXT/2

KEY

H	Overburden depth
B	Abutment angle
WT	Width of active mining zone
GEXT	Gob extent

Figure 6.—Illustration of the effect of panel geometry on the front abutment loading in ARMPS. A, gob area is supercritical in both width and extent; B, gob area is subcritical in extent; C, gob area is subcritical in width.

and 0.5, a portion of its abutment load is transferred to the AMZ. If the SF is less than 0.5, all of the additional side abutment load (but not the development or front abutment load) is transferred to the AMZ.

The final sources of load on the AMZ are the remnant barrier pillars inby the pillar line (between the front and side gobs). If the remnant barriers are too small to carry their load, some part of it is returned to the AMZ. The decision to transfer the load and how much is based on the remnant barrier's SF. Slabbing of the remnant will also return some abutment load to the AMZ.

Further details on the formulas and calculations used in ARMPS loadings can be found in the "Help" text that accompanies version 4.0 of the program.

VERIFICATION OF THE ARMPS METHOD

The ARMPS method is being verified through back-analysis of pillar recovery case histories. To date, 140 case histories have been obtained from 10 States (see appendix B of this paper). They cover an extensive range of geologic conditions, roof rock cavability characteristics, extraction methods, depths of cover, and pillar geometries. Ground conditions in each case history have been categorized as either satisfactory or unsatisfactory. Pillar failures responsible for unsatisfactory conditions were found to include—

• Pillar squeezes, accompanied by significant entry closure and loss of reserves;

• Sudden collapses of groups of pillars, usually accompanied by airblasts; and/or

• Coal pillar bumps (violent failures of one or more pillars).

As figure 7 shows, pillar failures occurred in 93% of the cases where the ARMPS SF was less than 0.75. Where the ARMPS SF was greater than 1.5, 94% of the designs were satisfactory. SF values ranging from 0.75 to 1.50 form a "gray" area where both successful and unsuccessful cases are found.

Current research has begun to evaluate other factors that may contribute to satisfactory conditions when the ARMPS SF falls between 0.75 and 1.5. These include—

Coal strength: An extensive data base of laboratory tests of the strength of coal was compiled by Mark and Barton [1997]. When compared with the ARMPS data base, no correlation was found between coal strength and pillar strength.

Depth of cover: Figure 8 shows that there is a marked reduction in SF as depth of cover increases. When the depth exceeds 305 m (1,000 ft), the ARMPS SF was below 1.0 for 70% of the satisfactory designs. Highly unsatisfactory conditions have also been encountered under deep cover, which recently led to two fatalities. Pillar design for retreat mining under deep cover remains an important research issue.

Seam height: A plot of seam height against ARMPS SF shows no correlation (figure 9).

Roof geology: A detailed study of pillar performance was conducted at a mining complex in southern West Virginia. More than 50 case histories were collected. Analysis showed that satisfactory conditions were more likely to be encountered under shale roof than massive sandstone roof (figures 10-11). This implies that better caving occurs with shale, resulting in lower pillar loads.
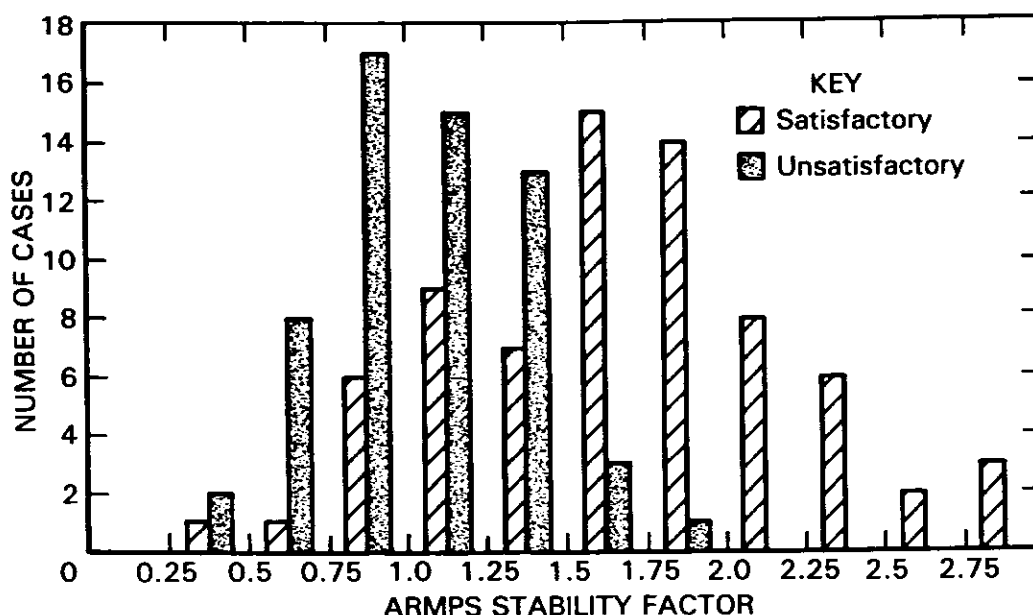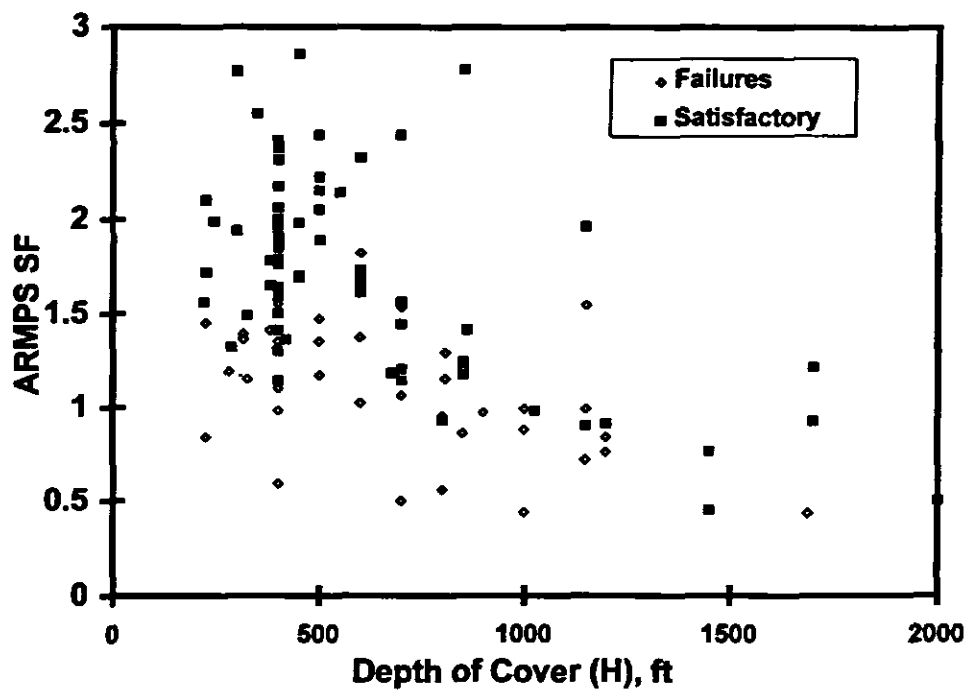

Figure 7.—ARMPS data base.

Figure 8.—Relationship between ARMPS SF and depth of cover within the case history data base.
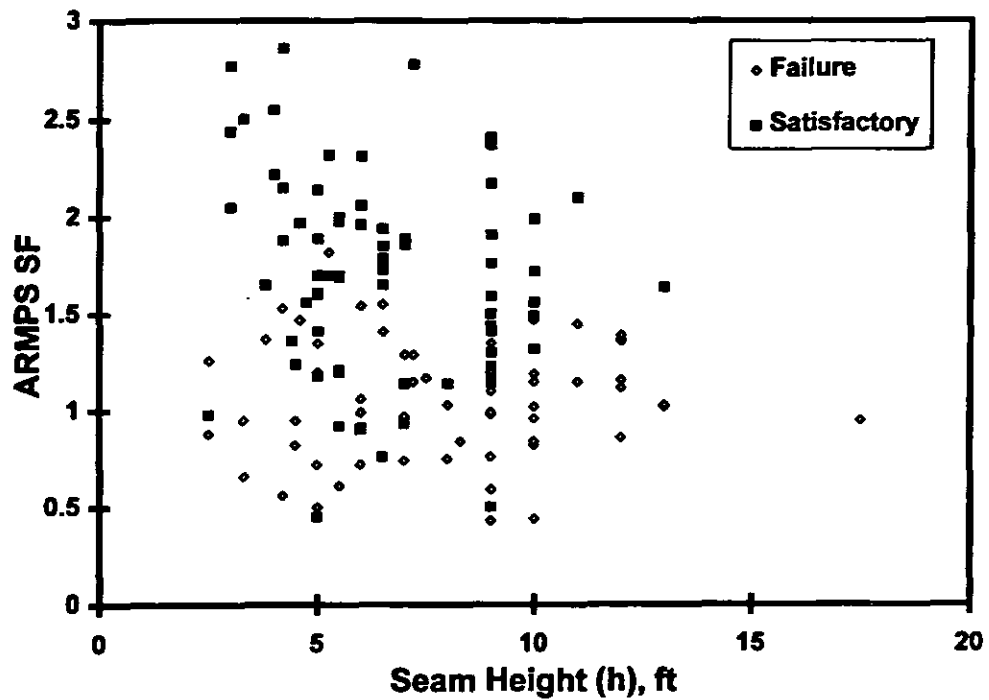

Figure 9.—Relationship between ARMPS SF and seam height within the case history data base.
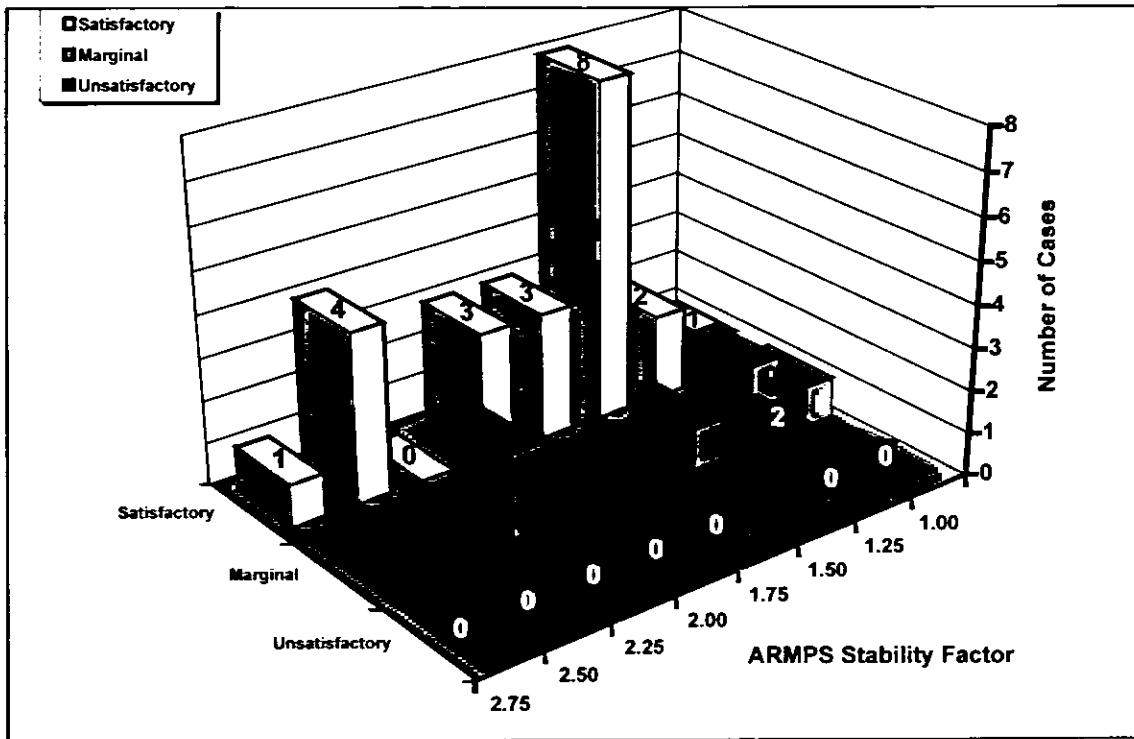
Figure 10.—Shale roof case histories from mining complex in southern West Virginia.
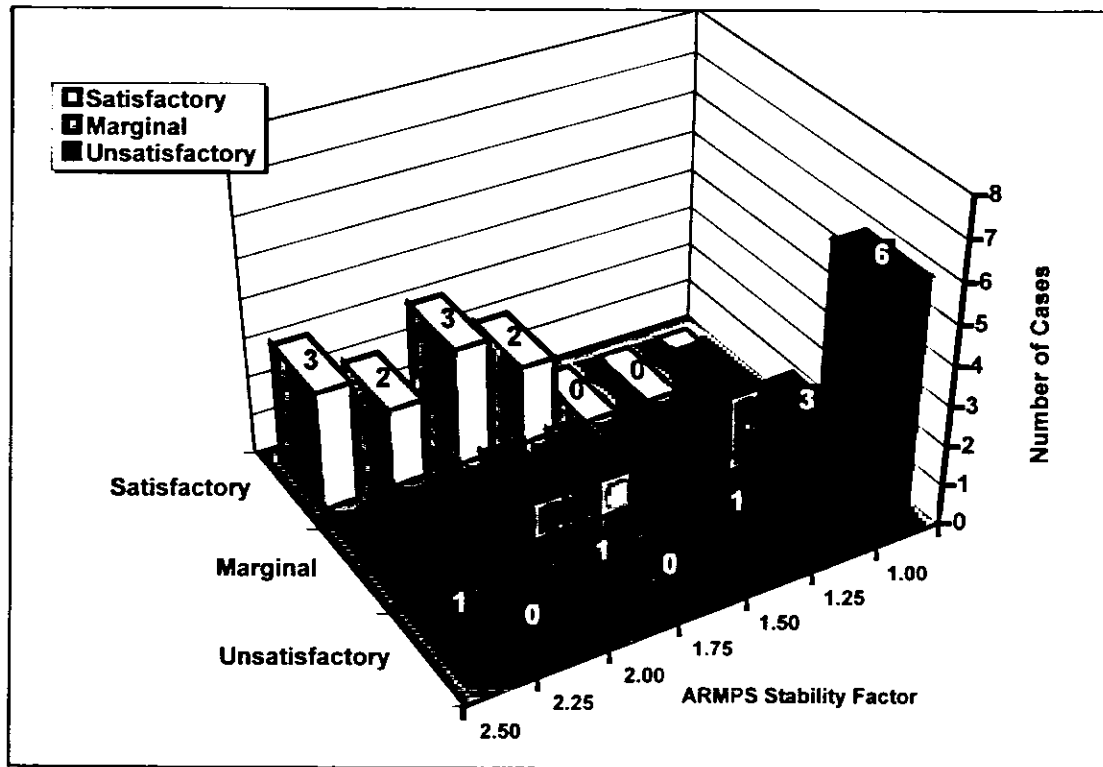

Figure 11.—Sandstone roof case histories from mining complex in southern West Virginia.

GUIDELINES FOR USING ARMPS

ARMPS appears to provide good first approximations of the pillar sizes required to prevent pillar failure during retreat mining. In an operating mine, past experience can be incorporated directly into ARMPS. ARMPS stability factors can be back-calculated for both successful and unsuccessful areas. Once a minimum ARMPS SF has been shown to provide adequate ground conditions, that minimum should be maintained in subsequent areas as changes occur in the depth of cover, coal thickness, or pillar layout. In this manner, ARMPS can be calibrated using site-specific experience.

ARMPS is also well suited for initial feasibility studies where no previous experience is available. Operators may begin with an SF near 1.5, then adjust as they observe pillar performance. ARMPS may also help in optimizing panel designs by identifying pillars that might be needlessly oversized.

ARMPS may be used to analyze a wide variety of mining geometries. For example, most bleeder designs can be analyzed by selecting loading condition 3, then setting the extent of the active gob to zero. The "Help" text included with version 4.0 of the program contains many tips on selecting the proper input parameters when using ARMPS.

In some cases, more detail may be desired than can be provided by ARMPS. Some complex situations, such as multiple-seam interactions, are beyond the capabilities of ARMPS. In these instances, the newly developed LAMODEL [Heasley 1997] may be the appropriate tool to use.

CONCLUSIONS

The ARMPS program has already proven to be a useful aid in planning pillar recovery operations. It is easy to use, and a large number of analyses can be run in a relatively short period. The program is sufficiently flexible to be applicable to a wide variety of mining geometries. If the user desires, it also provides a full range of intermediate calculations in addition to the SF. Many mines throughout the United States and abroad already use ARMPS, and the Mine Safety and Health Administration has also made extensive use of the program.

Current efforts are aimed at improving the interpretation of the ARMPS SF. Although pillar failures seem unlikely when the ARMPS SF is greater than 1.5, there are apparently many cases where SF values as low as 0.75 have been successful. Factors such as roof quality, floor strength, and mining method may determine whether a pillar design succeeds. These factors are now being included in the retreat mining case history data base and will be integrated into future design guidelines.

To obtain a single copy of the ARMPS computer program, version 4.0 for Windows, send three double-sided, high-density diskettes to: Christopher Mark, Ph.D., NIOSH, Pittsburgh Research Center, Cochrans Mills Rd., P.O. Box 18070, Pittsburgh, PA 15236-0070.

REFERENCES

Blaiklock J [1992]. A Kentuckian vote for continuous mining. Mining Magazine June:365-366.

Chase FE, Mark C [1993]. Ground control design for pillar extraction. Soc Min Eng AIME preprint 93-282.

Heasley KA [1997]. A new laminated overburden model for coal mine design. In: Mark C, Tuchman RJ, comp. Proceedings: New Technology for Ground Control in Retreat Mining. Pittsburgh, PA: U.S. Department of Health and Human Services, Public Health Service, Centers for Disease Control, National Institute for Occupational Safety and Health, IC 9446.

Mark C [1990]. Pillar design methods for longwall mining. Pittsburgh, PA: U.S. Department of the Interior, Bureau of Mines, IC 9247.

Mark C [1992]. Analysis of longwall pillar stability (ALPS): an update. In: Iannacchione AT, Mark C, Repsher RC, Tuchman RJ, Jones CC, comp. Proceedings of the Workshop on Coal Pillar Mechanics and Design. Pittsburgh, PA: U.S. Department of the Interior, Bureau of Mines, IC 9315, pp. 238-249.

Mark C, Barton TM [1997]. Pillar design and coal strength. In: Mark C, Tuchman RJ, comp. Proceedings: New Technology for Ground Control in Retreat Mining. Pittsburgh, PA: U.S. Department of Health and Human Services, Public Health Service, Centers for Disease Control, National Institute for Occupational Safety and Health, IC 9446.

APPENDIX A.—DERIVATION OF THE MARK-BIENIAWSKI PILLAR STRENGTH FORMULA

Early versions of the ARMPS program, following the ALPS program, used the Bieniawski formula to estimate pillar strength [Bieniawski 1992]:

$$S_p = S_1 [0.64 + (0.36 \, w/h)], \qquad \text{(A-1)}$$

where S_p =   pillar strength,

S_1 =   in situ coal strength,

w   =   pillar width (or least plan dimension),

and   h   =   pillar height.

The Bieniawski formula was originally developed in the 1960's from in situ testing of large-scale coal specimens. The specimen strengths were determined as the ultimate load-bearing capacity divided by the area. Bieniawski recognized that the formula underestimated the strength of rectangular pillars; however, because all of the specimens were square, there was no obvious way of estimating a "pillar length" effect.

It has been recognized that a major disadvantage of empirical formulas, like that of Bieniawski, is that they treat the pillar as a single structural element. In reality, the stress within even a relatively small pillar is highly nonuniform. Tests conducted by Wagner [1974] demonstrated this quite dramatically (figure A-1).

Modern *mechanics-based* approaches to coal pillars begin with stress distribution. Perhaps the best known is the approach proposed by Wilson [1973, 1983]. Wilson derived an expression for the vertical stress gradient within the yield zone, which he then integrated over the area of the pillar (figure A-2) to determine the ultimate pillar resistance (R). The "pillar strength" is simply the ultimate pillar resistance divided by the pillar area. Numerical models also provide stress distribution profiles, although not normally in the form of an equation. Mechanics-based approaches can be used to evaluate any pillar shape, because the stresses within the pillar are determined by laws that are independent of overall pillar geometry.

Although empirical formulas do not explicitly consider the effect of internal pillar mechanics, it is apparent that they imply a nonuniform stress distribution because of the shape effect. Once the implied stress gradient has been derived, the length effect can be readily determined. The derivation has been published previously [Mark et al. 1988; Mark and Iannacchione 1992] and is summarized below.

First, three assumptions are implicit in Wilson's and other analytical formulations:

1. The stress within the yield zone of a given pillar is a continuous function of the distance from the nearest rib.

2. The stress gradient within the yield zone of a given pillar does not change with time or load (i.e., the yielded coal is perfectly plastic).

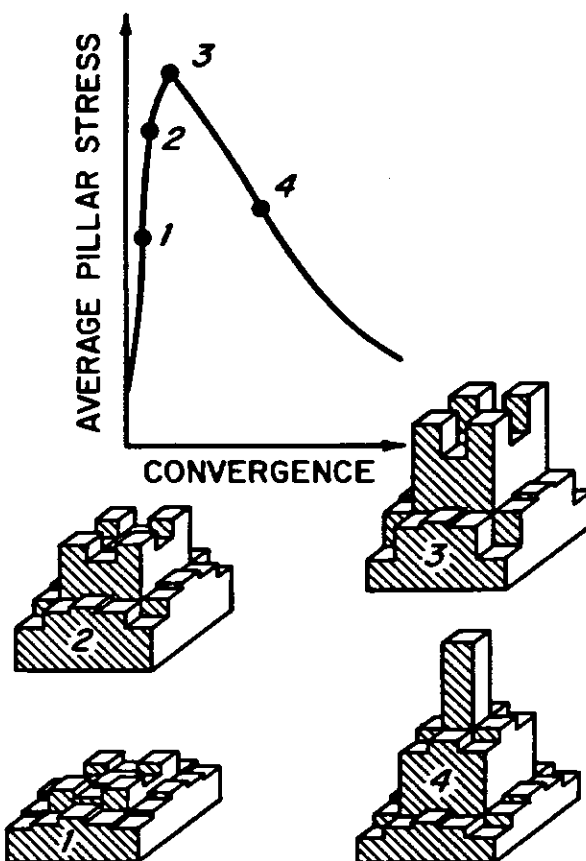3. The stress distribution is symmetric with respect to the center of the pillar.

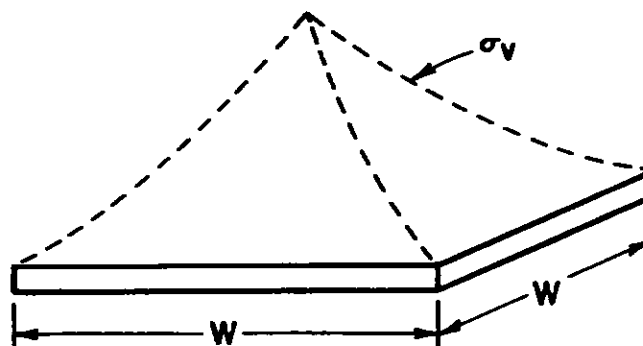Figure A-1.—Pillar stress profiles measured in small coal pillars (after Wagner [1974]).

Figure A-2.—Determination of pillar load-bearing capacity as the integral of the pillar stress distribution.

The next step in the derivation is to calculate the ultimate resistance of a square pillar. Using the Bieniawski formula:

$$R = S_1 \left(0.64 + 0.36 \frac{w}{h} \right) w^2. \qquad \text{(A-2)}$$

Then, the increase in pillar resistance dR due to an increase in cross-sectional area dA = 2w dw (figure A-3A) may be calculated by taking the derivative of equation A-2 with respect to w:

$$dR = S_1 \left(1.28 + 1.08 \frac{w^2}{h} \right) dw. \qquad \text{(A-3)}$$

In the next step, the assumption that the vertical pillar stress is a continuous function of the rib distance (x) is applied. It may be seen (figure A-3B) that

$$dR = 4 \int_0^{\frac{w}{2}} \sigma_v \, dx \, dw. \qquad \text{(A-4)}$$

Equating A-3 and A-4 and simplifying, we have

$$S_1 \left(0.32 \, w + 0.27 \frac{w^2}{h} \right) = \int_0^{\frac{w}{2}} \sigma_v \, dx. \qquad \text{(A-5)}$$

The function that satisfies equation A-5 is

$$\sigma_v = S_1 \left(0.64 + 2.16 \frac{x}{h} \right). \qquad \text{(A-6)}$$

Equation A-6 is the stress gradient in the yield zone predicted by the Bieniawski formula. Stress gradients have also been derived for several other common empirical pillar strength formulas [Mark and Iannacchione 1992].
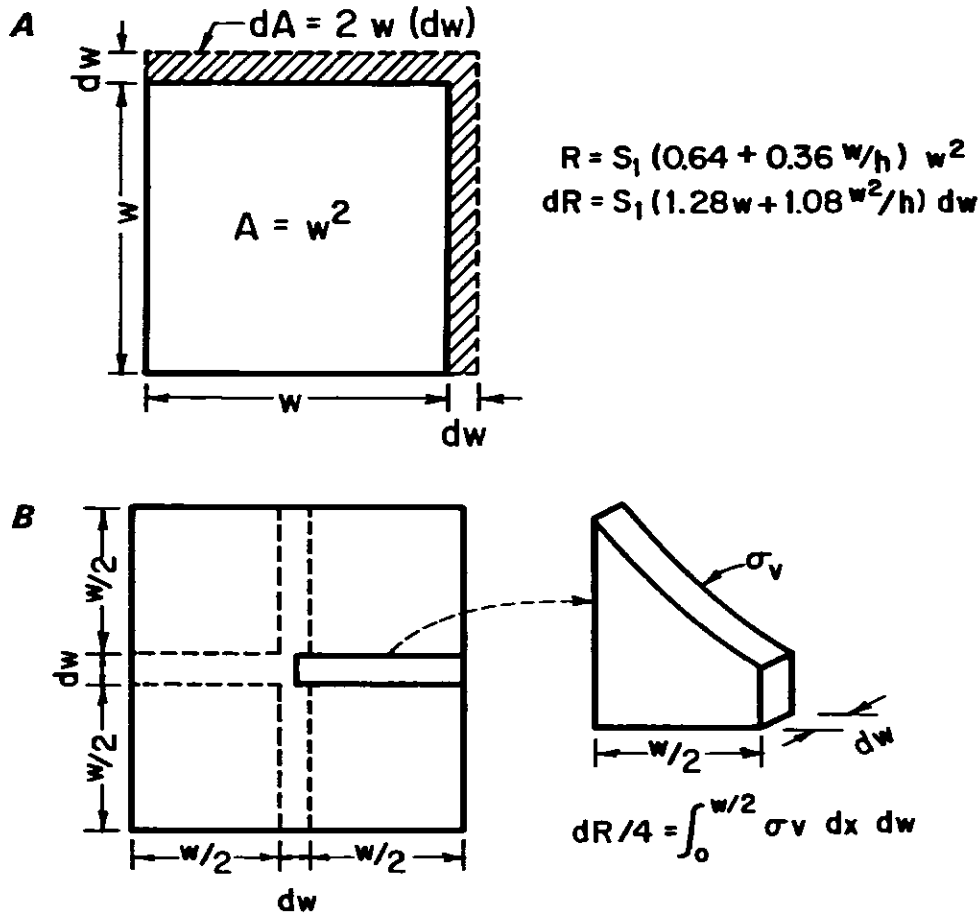

Figure A-3.—Determination of pillar stress gradients from a pillar strength formula. A, calculation of dR directly from the formula; B, calculation of dR in terms of the vertical stress gradient.

To determine the load-bearing capacity of any pillar shape, it is now only necessary to integrate equation A-6 over the load-bearing area of the pillar. For example, the load-bearing capacity of an extremely long strip pillar (R_s) is

$$R_s = 2L \int_0^{\frac{w}{2}} S_1 \left(0.64 + 2.16 \frac{x}{h} \right) dx. \qquad (A-7)$$

Solving:

$$R_s = (Lw) \, S_1 \left(0.64 + 0.54 \frac{w}{h} \right). \qquad (A-8)$$

Dividing by the pillar area (Lw) yields the strength of a strip pillar (S_s):

$$S_s = S_1 \left(0.64 + 0.54 \frac{w}{h} \right). \qquad (A-9)$$

Equation A-9 implies that a strip pillar's strength can approach 150% that of a square pillar, but that the strength difference is reduced as the w/h ratio is reduced.

The ultimate load carried by a rectangular pillar is equivalent to the load carried by a square pillar of width w plus a section of a strip pillar of length (L - w), as shown in figure A-4. Combining equations A-6 and A-9, the ultimate load carried by a rectangular pillar (R_s) is

$$R_s = S_1 \left\{ \left[w^2 \left(0.64 + 0.36 \frac{w}{h} \right) \right] + \left[(w(L-w)) \left(0.64 + 0.54 \frac{w}{h} \right) \right] \right\}. \qquad (A-10)$$

Simplifying:

$$R_s = S_1 \left[0.64 \, wL + 0.54 \left(w^2 \frac{L}{h} \right) - 0.18 \left(\frac{w^3}{H} \right) \right]. \qquad (A-11)$$

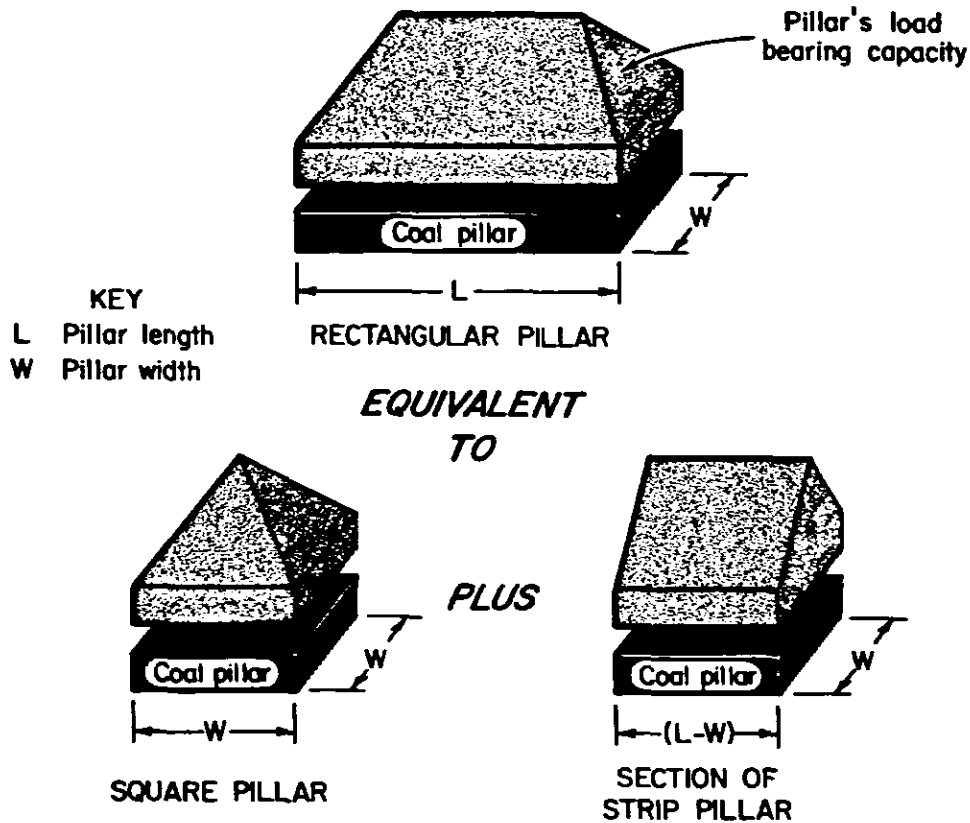KEY
L   Pillar length
W   Pillar width

Figure A-4.—Pillar stress distributions for square, strip, and rectangular pillars.

Dividing by the load-bearing area (wL), the Mark-Bieniawski formula is obtained:

$$S_p = S_1 \left[0.64 + 0.54 \left(\frac{w}{H} \right) - 0.18 \frac{w^2}{Lh} \right]. \qquad (A-12)$$

Equation A-12 indicates that the increase in strength in a rectangular pillar depends on both (w/h) and (w/L). Table A-1 compares the pillar strengths determined by the Mark-Bieniawski formula with those obtained from the Bieniawski formula.

Table A-1.—Pillar strength from the Mark-Bieniawski formula, assuming the strength of a square pillar (original Bieniawski formula) as unity

Pillar L/w	Pillar w/h				
	1	2	4	10	20
1.5	1.06	1.09	1.12	1.14	1.16
2.0	1.09	1.13	1.18	1.21	1.23
4.0	1.14	1.23	1.32	1.41	1.45
10.0	1.16	1.25	1.34	1.42	1.48

REFERENCES

Bieniawski ZT [1992]. A method revisited: coal pillar strength formula based on field investigations. In: Iannacchione AT, Mark C, Repsher RC, Tuchman RJ, Jones CC, comp. Proceedings of the Workshop on Coal Pillar Mechanics and Design. Pittsburgh, PA: U.S. Department of the Interior, Bureau of Mines, IC 9315, pp. 158-165.

Mark C, Iannacchione AT [1992]. Coal pillar mechanics: theoretical models and field measurements compared. In: Iannacchione AT, Mark C, Repsher RC, Tuchman RJ, Jones CC, comp. Proceedings of the Workshop on Coal Pillar Mechanics and Design. Pittsburgh, PA: U.S. Department of the Interior, Bureau of Mines, IC 9315, pp. 78-93.

Mark C, Listak JM, Bieniawski ZT [1988]. Yielding coal pillars—field measurements and analysis of design methods. In: Proceedings of the 29th U.S. Symposium on Rock Mechanics. Minneapolis, MN: University of Minnesota, pp. 261-270.

Wagner H [1974]. Determination of the complete load-deformation characteristics of coal pillars. In: Proceedings of the 3rd International Society for Rock Mechanics Congress. Denver, CO: pp. 1076-1081.

Wilson AH [1973]. An hypothesis concerning pillar stability. Min Eng (London) 131(141):409-417.

Wilson AH [1983]. The stability of underground workings in the soft rocks of the coal measures. Intl J Rock Mech Min Sci 1:91-187.

APPENDIX B.—ARMPS CASE HISTORY DATA BASE

Table B-1.—Unsatisfactory pillar retreat case histories

State and coal seam	ARMPS SF	Seam thickness, m (ft)	Depth, m (ft)	Loading condition
Alabama:				
Blue Creek	1.54	1.8 (6.0)	350 (1,150)	2
Blue Creek	0.99	1.8 (6.0)	350 (1,150)	3
Colorado:				
Cameo	0.74	2.1 (7.0)	90 (300)	1
D	1.20	2.7 (9.0)	260 (850)	2
D	0.99	2.7 (9.0)	305 (1,000)	3
Kentucky:				
Harlan	1.16	3.7 (12)	285 (940)	1
Harlan	0.96	2.1 (7.0)	305 (1,000)	1
Harlan	0.86	3.7 (12)	260 (850)	2
Harlan	1.12	3.7 (12)	325 (1,070)	1
Hazard No. 4	0.44	3.0 (10)	305 (1,000)	4
Hazard No. 4	0.56	1.3 (4.2)	245 (800)	3
Hazard No. 4	0.50	1.5 (5.0)	215 (700)	3
Lower Elkhorn (No. 2 Gas)	1.03	4.0 (13.0)	245 (800)	1
Lower Elkhorn (No. 2 Gas)	1.02	4.0 (13.0)	185 (600)	3
Ohio:				
Lower Freeport	1.20	1.5 (5.0)	215 (700)	1
Mahoning	0.66	1.0 (3.3)	75 (250)	1
Mahoning	0.95	1.0 (3.3)	75 (250)	1
Pennsylvania:				
Lower Kittanning	1.41	2.0 (6.5)	115 (380)	2
Lower Kittanning	1.55	2.0 (6.5)	120 (400)	2
Lower Kittanning	1.29	2.1 (7.0)	75 (250)	1
Pittsburgh	0.97	2.1 (7.0)	275 (900)	3
Pittsburgh	1.17	2.3 (7.5)	150 (500)	3
Pittsburgh	1.29	2.2 (7.2)	245 (810)	4
Pittsburgh	1.15	2.2 (7.2)	245 (810)	4
Sewickley	1.82	1.6 (5.25)	185 (600)	3
Tennessee:				
Beach Grove	1.26	0.8 (2.5)	315 (1,025)	1
Beach Grove	0.88	0.8 (2.5)	305 (1,000)	3
Utah:				
Blind Canton	0.84	2.5 (8.3)	365 (1,200)	3
Gilson	0.76	2.7 (9.0)	365 (1,200)	3
Gilson	0.43	2.7 (9.0)	515 (1,690)	3
Lower O'Connor	0.95	5.3 (17.5)	170 (550)	1
Virginia:				
Blair	1.37	1.2 (3.8)	185 (600)	3
Glamorgan	1.06	1.8 (6.0)	215 (700)	3
Jawbone	1.53	1.3 (4.2)	215 (700)	3
Jawbone	1.47	1.4 (4.6)	150 (500)	3
Pocahontas No. 3	0.61	1.7 (5.5)	520 (1,700)	1
Pocahontas No. 3	1.35	1.5 (5.0)	150 (500)	3
Pocahontas No. 4	1.03	2.4 (8.0)	90 (300)	1
West Virginia:				
Beckley	0.72	1.8 (6.0)	350 (1,150)	4
Coalburg	0.75	2.4 (8.0)	90 (300)	1
Coalburg	0.59	2.7 (9.0)	120 (400)	NAp
Coalburg	0.98	2.7 (9.0)	120 (400)	NAp
Coalburg	1.10	2.7 (9.0)	120 (400)	NAp
Coalburg	1.35	2.7 (9.0)	120 (400)	NAp

See explanatory notes at end of table.

Table B-1.—Unsatisfactory pillar retreat case histories—Continued

State and coal seam	ARMPS SF	Seam thickness, m (ft)	Depth, m (ft)	Loading condition
West Virginia:—Continued				
Dorothy	1.36	3.7 (12.0)	95 (315)	3
Dorothy	1.37	3.7 (12.0)	95 (315)	2
Dorothy (Winifrede)	1.15	3.4 (11.0)	70 (225)	1
Dorothy (Winifrede)	1.45	3.4 (11.0)	70 (225)	4
Dorothy (Winifrede)	1.39	3.7 (12.0)	95 (315)	2
Dorothy (Winifrede)	1.02	3.0 (10.0)	55 (175)	1
Dorothy (Winifrede)	1.15	3.0 (10.0)	100 (325)	2
No. 2 Gas	0.95	1.4 (4.5)	245 (800)	4
Stockton	0.84	3.0 (10.0)	70 (225)	2
Stockton	0.96	3.0 (10.0)	75 (240)	1
Stockton	0.82	3.0 (10.0)	75 (245)	1
Stockton	1.47	3.0 (10.0)	85 (280)	1
Stockton	1.19	3.0 (10.0)	85 (280)	2
([1])	0.72	1.5 (5.0)	120 (400)	1
([1])	0.82	1.4 (4.5)	115 (375)	1

NAp   Not applicable.
[1]Not provided by original reference.

Table B-2.—Satisfactory pillar retreat case histories

State and coal seam	ARMPS SF	Seam thickness, m (ft)	Depth, m (ft)	Loading condition
Alabama:				
Blue Creek	1.96	1.8 (6.0)	350 (1,150)	2
Colorado:				
Cameo	1.86	2.1 (7.0)	120 (400)	3
Cameo	1.14	2.1 (7.0)	215 (700)	2
Cameo	0.93	2.1 (7.0)	245 (800)	3
D	1.23	2.7 (9.0)	260 (850)	2
D	1.44	2.7 (9.0)	215 (700)	2
Illinois:				
Herrin No. 6	1.14	2.4 (8.0)	215 (700)	3
Kentucky:				
Harlan	1.94	2.0 (6.5)	90 (300)	3
Hazard No. 4	1.36	1.3 (4.4)	130 (420)	3
Kellioka	1.41	1.5 (5.0)	260 (860)	2
Kellioka	1.18	1.5 (5.0)	205 (675)	3
Kellioka	0.45	1.5 (5.0)	440 (1,450)	3
Kellioka	1.61	1.5 (5.0)	185 (600)	3
Lower Elkhorn (No. 6 Gas)	1.64	4.0 (13.0)	120 (400)	3
Pond Creek	1.20	1.7 (5.5)	215 (700)	2
Pond Creek	1.70	1.7 (5.5)	135 (450)	3
Pond Creek	2.0	1.7 (5.5)	120 (400)	2
Pond Creek	1.98	1.7 (5.5)	135 (450)	3
Pond Creek	1.69	1.7 (5.5)	135 (450)	2
Ohio:				
Lower Freeport	1.60	1.5 (5.0)	170 (550)	1
Lower Freeport	1.70	1.5 (5.0)	170 (550)	1
Mahoning	2.50	1.0 (3.3)	75 (250)	1
Pennsylvania:				
Lower Freeport	2.06	1.8 (6.0)	120 (400)	3
Lower Kittanning	1.65	2.0 (6.5)	115 (380)	3
Lower Kittanning	1.78	2.0 (6.5)	115 (380)	3
Lower Kittanning	1.79	2.0 (6.5)	120 (400)	3
Lower Kittanning	1.85	2.0 (6.5)	120 (400)	2
Lower Kittanning	2.14	1.5 (5.0)	170 (550)	3
Pittsburgh	1.89	2.1 (7.0)	150 (500)	3
Pittsburgh	2.78	2.2 (7.2)	260 (855)	2
Sewickley	1.70	1.6 (5.25)	185 (600)	3
Sewickley	2.32	1.6 (5.25)	185 (600)	2
Upper Freeport	1.88	1.3 (4.2)	65 (210)	1
Tennessee:				
Beach Grove	0.98	0.8 (2.5)	315 (1,025)	2
Utah:				
Gilson	0.50	2.7 (9.0)	610 (2,000)	2
Virginia:				
Blair	1.65	1.2 (3.8)	185 (600)	3
Glamorgan	2.31	1.8 (6.0)	120 (400)	3
Jawbone	2.86	1.3 (4.2)	135 (450)	2
Jawbone	2.15	1.3 (4.2)	150 (500)	3
Jawbone	1.97	1.4 (4.6)	120 (400)	3
Mossy-Haggy	2.05	0.9 (3.0)	150 (500)	3
Pocahontas No. 3	0.92	1.7 (5.5)	520 (1,700)	2
Pocahontas No. 3	1.21	1.7 (5.5)	520 (1,700)	3
Pocahontas No. 3	1.89	1.5 (5.0)	150 (500)	2
Pocahontas No. 4	0.91	1.8 (6.0)	365 (1,200)	3
Pocahontas No. 4	2.77	0.9 (3.0)	90 (300)	2
Pocahontas No. 4	0.76	2.0 (6.5)	440 (1,450)	3
Red Ash	2.44	0.9 (3.0)	150 (500)	2
Red Ash	2.44	0.9 (3.0)	215 (700)	3
Tiller	2.22	1.2 (4.0)	150 (500)	3

See explanatory notes at end of table.

Table B-2.—Satisfactory pillar retreat case histories—Continued

State and coal seam	ARMPS SF	Seam thickness, m (ft)	Depth, m (ft)	Loading condition
West Virginia:				
Beckley	0.90	1.8 (6.0)	350 (1,150)	4
Beckley	1.17	2.7 (9.0)	260 (850)	4
Coalburg	1.14	2.7 (9.0)	120 (400)	NAp
Coalburg	1.30	2.7 (9.0)	120 (400)	NAp
Coalburg	1.41	2.7 (9.0)	120 (400)	NAp
Coalburg	1.50	2.7 (9.0)	120 (400)	NAp
Coalburg	1.59	2.7 (9.0)	120 (400)	NAp
Coalburg	1.76	2.7 (9.0)	120 (400)	NAp
Coalburg	1.91	2.7 (9.0)	120 (400)	NAp
Coalburg	2.17	2.7 (9.0)	120 (400)	NAp
Coalburg	2.37	2.7 (9.0)	120 (400)	NAp
Coalburg	2.41	2.7 (9.0)	120 (400)	NAp
Dorothy (Winifrede)	2.10	3.4 (11.0)	70 (225)	2
Dorothy (Winifrede)	1.32	3.0 (10.0)	85 (285)	2
Dorothy (Winifrede)	1.49	3.0 (10.0)	100 (325)	2
Dorothy (Winifrede)	1.72	3.0 (10.0)	70 (225)	2
Fire Creek	1.24	1.4 (4.5)	260 (850)	2
Lower Winifrede	1.73	2.0 (6.5)	185 (600)	2
Peerless	1.56	1.4 (4.75)	215 (700)	2
Sewell	2.55	1.2 (4.0)	105 (350)	2
Stockton	1.56	3.0 (10.0)	65 (220)	2
Stockton	1.99	3.0 (10.0)	75 (245)	2

NAp   Not applicable.

PREVENTING MASSIVE PILLAR COLLAPSES
IN COAL MINES

By Christopher Mark, Ph.D,[1] Frank E. Chase,[2] and R. Karl Zipf, Jr., Ph.D.[3]

ABSTRACT

A massive pillar collapse occurs when undersized pillars fail and rapidly shed their load to adjacent pillars, which in turn fail. The consequences of these chain-reaction failures can be catastrophic. One effect of a massive pillar collapse can be a powerful, destructive, and potentially hazardous airblast. Thirteen recent massive pillar collapses have been documented in West Virginia, Ohio, Utah, and Colorado. Data collected at the failure sites indicate that all of the massive collapses occurred where the pillar width-to-height (w/h) ratio was 3.0 or less and where the Analysis of Retreat Mining Pillar Stability Factor was less than 1.5. The unique structural characteristics of these pillar systems apparently result in sudden, massive pillar failures, rather than the more common slow "squeezes." The field data, combined with theoretical analysis, provide the basis for two partial-extraction design approaches to control massive pillar collapses. These are the *containment* approach and the *prevention* approach; practical examples are provided of each.

[1]Mining engineer, Pittsburgh Research Center, National Institute for Occupational Safety and Health, Pittsburgh, PA.
[2]Geologist, Pittsburgh Research Center, National Institute for Occupational Safety and Health, Pittsburgh, PA.
[3]Lecturer, Department of Mining and Metallurgical Engineering, University of Queensland, Brisbane, Queensland, Australia.

INTRODUCTION

Massive pillar collapses in room-and-pillar mines have also been labeled "cascading pillar failures," "domino-type failures," or "pillar runs." In this type of failure, when one pillar collapses, the load that it carried transfers rapidly to its neighbors, causing them to fail, and so forth. This failure mechanism can lead to the rapid collapse of very large mine areas. In mild cases, only a few tens of pillars might fail; however, in extreme cases, hundreds, even thousands, of pillars can collapse.

Massive pillar collapses can have catastrophic effects on a mine. Sometimes these effects pose a greater safety risk than the underlying ground control problem. Usually, the collapse induces a devastating airblast due to the displacement of air from the collapsed area. An airblast can totally disrupt the ventilation system at a mine by destroying ventilation stoppings, seals, and fan housings. Flying debris can seriously

injure or kill mining personnel. The collapse might also fracture a large volume of rock in the pillars and immediate roof and floor. In coal and other gassy mines, this fragmentation can lead to the sudden release of large quantities of methane gas into the mine atmosphere, creating an explosion hazard. Finally, a massive pillar collapse can release significant seismic energy that may be experienced on the surface as a small earthquake.

Fortunately, not all pillar failures are sudden, massive collapses. Most are slow "squeezes" that develop over days to weeks, and because of their slow progress, do not pose as great a danger to mining personnel. A central goal of the research described in this paper was to identify the physical characteristics that distinguish sudden collapses from other pillar failures.

CASE HISTORIES

The most infamous massive pillar collapse in history occurred in 1960 at Coalbrook North Colliery in South Africa. Thousands of 12- by 12- by 4.2-m (40- by 40- by 14-ft) pillars collapsed over a 305-ha (750-acre) area in 5 min, killing 437 miners [Bryan et al. 1966]. Numerous other, smaller collapses have been reported in South Africa since then [Madden 1991]. In Australia, the New South Wales Joint Coal Board reported eight massive pillar collapses between 1990 and 1993 [University of New South Wales School of Mines 1994].

Massive collapses have also occurred in metal and nonmetal mines. Zipf and Mark [1996] documented six examples from lead-zinc, copper, silica, and salt mines. The largest occurred at a Wyoming trona mine in 1995, where 160 ha (400 acres) of 4- by 29- by 6-m (13- by 95- by 19-ft) fenders collapsed, resulting in a Richter magnitude 5.3 earthquake and one fatality underground [Ferriter et al. 1996]. The ventilation system at the mine was heavily damaged, and an estimated 1 million m^3 (30 million ft^3) of methane was liberated on the day of the collapse. Methane release levels did not return to normal until 3 months later [Ferriter et al. 1996].

In 1992, the former U.S. Bureau of Mines (USBM) was asked to investigate a massive pillar collapse and resultant destructive airblast that had occurred in a coal mine in Mingo County, WV. Subsequent investigations found 12 other examples, which were documented by field investigations [Chase et al. 1994]. Geotechnical evaluations examined the competency of the immediate roof, as well as that of the main roof and its susceptibility to caving. The Analysis of Retreat Mining Pillar Stability (ARMPS) program [Mark and Chase

1997] was used to determine the pillar stability factors (SF). Four examples that illustrate different mining methods and effects are described in detail below.

PILLAR SPLITTING (MINE A)

Mine A is located in Mingo County, WV, and is extracting the 2.9-m (9.5-ft) thick Coalburg Coalbed. A 28-m (90-ft) thick massive sandstone unit with a compressive strength of 83 MPa (12,000 psi) formed the roof above the collapsed area. The Coal Mine Roof Rating (CMRR) of the immediate roof was calculated to be 74. Below the noncleated coalbed is 10.5 m (34 ft) of competent sandy shale and sandstone units. All roadways were 6 m (20 ft) wide.

In 1991, the panel shown in figure 1 was developed. All roadways were driven on 18-m (60-ft) centers and were under 85 m (275 ft) of cover. After the panel was completed, partial pillar recovery was begun. A 6-m (20-ft) wide split was mined through the middle of each pillar, and two 3- by 12-m (10- by 40-ft) fenders with an ARMPS SF of 0.75 remained. Because of the competency of the roof and the support provided by the regularly spaced uniform fenders, no caving occurred while the panel was being retreat mined. Three weeks after the panel had been abandoned, an area measuring approximately 140 by 155 m (450 by 500 ft) containing 107 fenders collapsed. Miners on a nearby section were knocked to the floor by the resultant airblast. One miner was bounced off of a steel rail and required 26 stitches to his head. Fortunately, no miners were near the collapse. However, if the failure had occurred 15 min later, two miners would have
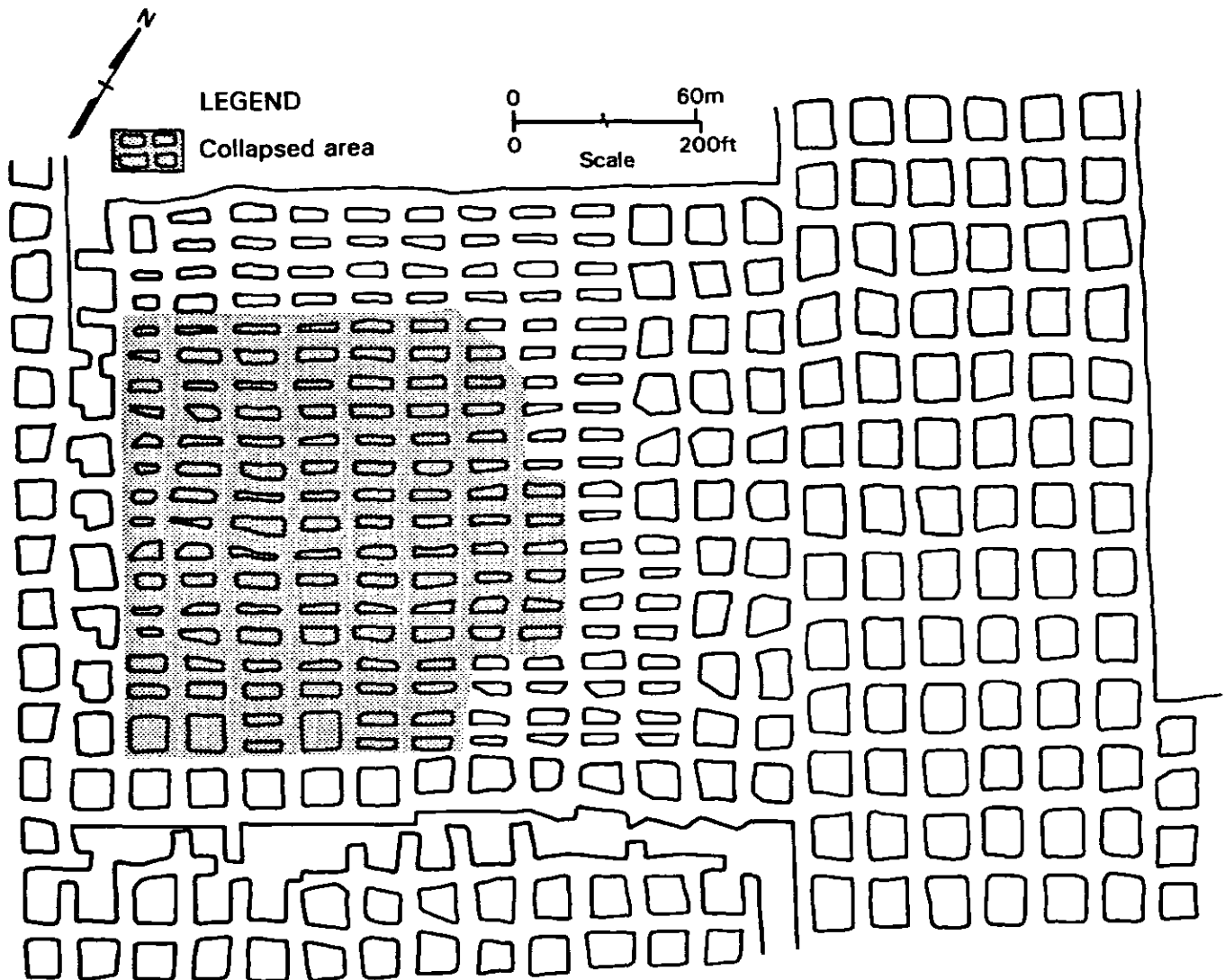
Figure 1.—Failed split-pillar workings in Mine A.

been rock dusting ribs immediately outby the area that collapsed. The airblast blew out 26 cinder block stoppings and the fan house weak wall, which closed the mine for days.

As was the case in many of the other collapses that were studied, a number of fenders near the edge of the collapse did not fail. There are two possible explanations for this: (1) The collapse might terminate as soon as the competent roof units were able to bridge the span, or (2) the collapse might terminate where the fenders were shielded from the full load by the adjacent abutment. In the second case, the 12- by 12-m (40- by 40-ft) pillars with an SF of 2.33 may have provided a hinge line, which allowed the roof to cantilever over the first several rows of fenders.

An earlier collapse had occurred at Mine A in partially pillared workings under very similar conditions. Damage was

limited to blown out stoppings, and no one was injured. Complete documentation of this case was unavailable.

After the second collapse, the practice of pillar splitting was reexamined at the mine. Several sets of mobile roof supports were purchased, and retreat mining continued with full pillar extraction. Most recently, some pillar splitting has been conducted, with rows of unsplit pillars left as barriers to isolate retreated areas.

PILLAR SPLITTING/ABUTMENT LOAD OVERRIDE (MINE C)

Mine C is located in Logan County, WV, and is extracting the 3-m (10-ft) thick Dorothy Coalbed. The immediate and main roof throughout the mine is composed of a fine-grained,

semilaminated sandstone with a CMRR of 64; the floor was composed of an extremely firm sandstone. Coalbed cleating was nonexistent. All roadways in the mine were 6 m (20 ft) wide and were driven on 18-m (60-ft) centers in the relevant area.

In 1992, the operator was splitting pillars in the panel shown in figure 2. After the 6-m (20-ft) wide split, two 3- by 12-m (10- by 40-ft) fenders with an SF of 0.94-1.15 remained. When the operator began to mine the pillar row outby the last row split (figure 2), a massive collapse of the fenders in the gobbed-out area initiated. The roof bolter operator on the section indicated that he and his coworkers were knocked to the floor by the resulting airblast, and 103 stoppings were destroyed. The pillars where the collapse terminated had an SF of 1.97. Overburden in the collapsed area ranged from 53 to 66 m (175 to 215 ft).

A subsequent pillar collapse occurred at Mine C, apparently triggered by time deterioration and front abutment pressures generated by full pillar extraction. Roadways in the collapsed area were driven on 15-m (50-ft) centers, and 91 pillars with an SF of 1.08 failed. Pillars with an SF of 1.69 halted the collapse. These roadways were driven on 18-m (60-ft) centers. No stoppings were damaged, and the overburden in the area was 99 m (325 ft).

Mine C was visited in February 1994 to observe diagonal pillar splitting, which is not a common practice. Roadways were driven on 15-m (50-ft) centers, and the pillar splits were 5 m (16 ft) wide. The extraction percentage was 86%. The triangular remnant stumps were observed to routinely crush out after finishing the pillar row, and the roof caved immediately inby the breakers. The breakers and wedges

showed no weight. Where the first pillar collapse occurred in Mine C using the traditional 6-m (20-ft) wide split through a 12- by 12-m (40- by 40-ft) pillar, 78% of the coal was extracted. This 8% increase in resource recovery, coupled with a less stable triangular stump with a smaller perimeter, probably explains why the roof caves more readily than in traditional pillar splitting.

SMALL-CENTER MINING (MINE D)

Mine D is located in Mingo County, WV, and is extracting the 3.4-m (11-ft) thick Dorothy Coalbed. The roof consisted of 76 cm (2.5 ft) of laminated fossiliferous shale and 7 cm (3 in) of rider coal, and 25 m (80 ft) of cross-bedded sandstone was observed in the highwall. The roof had a CMRR of 81. Below the noncleated coalbed was 1.5 m (5 ft) of sandy shale and 28 m (91 ft) of sandstone. All roadways in the mine were 6 m (20 ft) wide.

In 1992, ninety-four 6- by 6-m (20- by 20-ft) pillars with an SF of 1.15 and thirty-two 9- by 9-m (30- by 30-ft) pillars with an SF of 1.45 failed. As shown in figure 3, the pillar failures occurred in a panel driven off the mains. The resultant airblast blew out 37 stoppings. The only other stopping in the mine had a hole in it. Some of these stoppings were as far away as 244 m (800 ft) from the perimeter of the collapse. In one stopping, it was determined that some of its 14-kg (30-lb) cinder blocks had been hurled 152 m (500 ft). Fortunately, the occurrence was on an idle shift, and no one was in the mine. The collapse was halted by pillars in the main entries, which were 12- by 12-m (40- by 40-ft) and had an SF of 3.33. Cover over the collapsed area was 69 m (225 ft).
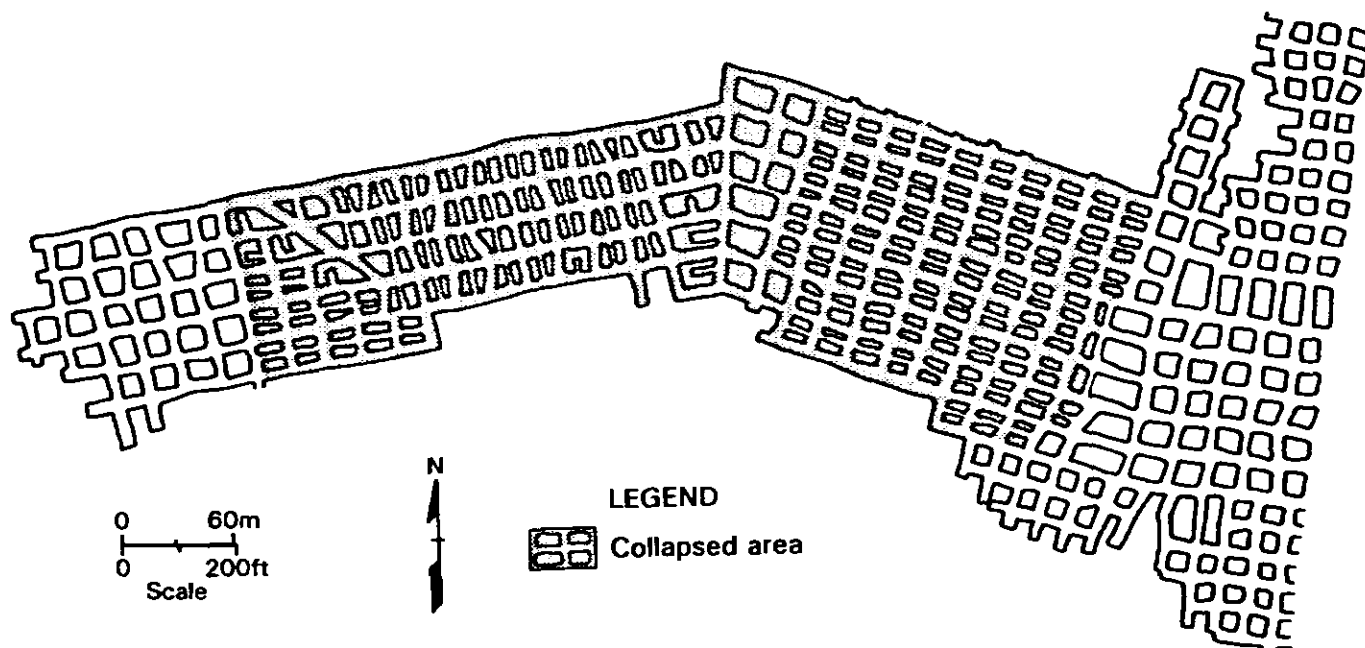

0   60m
0   200ft
Scale

N

LEGEND

Collapsed area

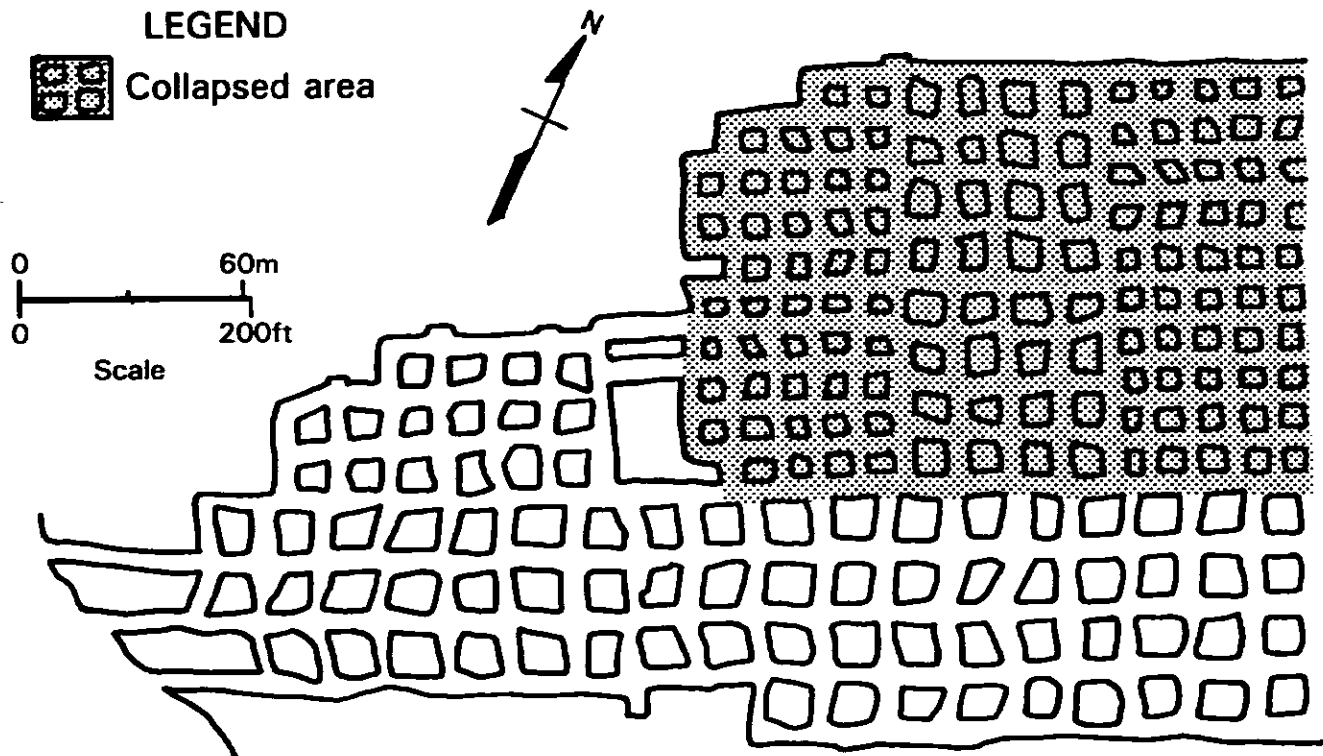Figure 2.—Location of split-pillar collapse at Mine C.

Figure 3.—Failed small-center development workings at Mine D.

FLOOR RECOVERY (MINE G)

Mine G is located in Utah and was extracting the 8-m (25-ft) thick Lower O'Connor Seam [Ropchan 1991]. There were previous workings in the Upper O'Connor above Mine G, separated by 18-23 m (60-80 ft) of overburden. The total overburden above the collapsed area was about 170 m (550 ft).

Room-and-pillar workings were advanced 2.4 m (8 ft) high on 18-m (60-ft) centers. The panel was developed nine entries wide and 535 m (1,740 ft) long. The pillars were not extracted on retreat, but an additional 3 m (10 ft) was removed from the floor, leaving 5.4-m (18-ft) high remnants. Mining the floor coal decreased the w/h ratio of the pillars from 5 to 2.2 and reduced their strength by about 45%.

The collapse occurred when the section was within two crosscuts of being completely retreated. The force of the airblast hurled three miners for distances of 12-30 m (40-100 ft), causing one severe head laceration. A 2-ton shop car was blown through a stopping. There was extensive damage to ventilation structures; concrete blocks from stoppings were scattered up to 30 m (100 ft). The main mine fan was stalled, and airflow in the mine was temporarily reversed. There was

some speculation that a north-south trending fault that bordered the panel may have contributed to the collapse.

SUMMARY OF CASE HISTORIES

Table 1 summarizes the mining dimensions of 13 examples of massive pillar collapses in U.S. coal mines. All occurred during the 1980's and 1990's, and all happened suddenly or without significant warning. Most resulted in airblasts and damage to the ventilation system.

Analysis of the data reveals some important similarities. First, the ARMPS SF was less than 1.5 in every case and less than 1.2 in 81% of the cases. This implies that the pillars were not sized to carry the full overburden load. Pillar failures are not unusual; however, most are slow and nonviolent. What apparently distinguishes the sudden collapses from the slow squeezes is the pillar's w/h ratio. Every massive pillar collapse involved *slender* pillars with a w/h ratio of less than 3. Another common characteristic of the collapses is that the overburden was judged to be relatively strong in every case. Finally, the collapsed areas were all at least 1.6 ha (4 acres), and the minimum dimension of a collapsed panel suffering major damage was 110 m (350 ft).

Table 1.—Massive pillar collapses in coal mines

Case history	State	Depth, m (ft)	Pillar size, m (ft)	ARMPS SF	w/h ratio	Collapsed area, ha (acres)	Collapse size, m (ft)	Damage from airblast
A	WV	84 (275)	3 by 12 (10 by 40)	0.86	1.05	2.3 (5.7)	150 by 150 (500 by 500)	28 stoppings, 1 injury.
B1	WV	73 (240)	3 by 12 (10 by 40)	0.96	1.00	—	—	32 stoppings, fan wall out.
			3 by 18 (10 by 60)	1.10	1.00			
B2	WV	75 (245)	3 by 12 (10 by 40)	0.94	1.00	1.7 (4.1)	100 by 150 (350 by 500)	40 stoppings.
B3	WV	85 (280)	9 by 9 (30 by 30)	1.46	3.00	2.8 (6.8)	180 by 180 (600 by 600)	70 stoppings.
			6 by 12 (20 by 40)	1.47	2.00			
C1	WV	60 (195)	3 by 12 (10 by 40)	1.19	1.00	2.1 (5.2)	140 by 150 (450 by 500)	103 stoppings.
C2	WV	99 (325)	9 by 9 (30 by 30)	1.15	3.00	1.9 (4.8)	100 by 180 (350 by 600)	Minimal.
D	WV	69 (225)	6 by 6 (20 by 20)	1.15	1.82	1.7 (4.3)	100 by 160 (350 by 540)	37 stoppings.
			9 by 9 (30 by 30)	1.42	2.73			
E1	WV	91 (300)	3 by 12 (10 by 40)	0.79	1.42	7.4 (18.2)	240 by 290 (800 by 950)	Major damage.
E2	WV	91 (300)	3 by 12 (10 by 40)	0.71	1.11	6.7 (16.6)	220 by 275 (720 by 900)	Major damage.
F	OH	76 (250)	2 by 12 (7 by 39)	0.66	2.12	2.0 (4.9)	90 by 215 (300 by 700)	Minimal.
G	UT	168 (550)	12 by 12 (40 by 40)	0.95	2.29	7.9 (19.4)	150 by 490 (480 by 1,620)	Major damage, 1 injury.
O	WV	—	—	1.03	2.50	1.8 (4.5)	120 by 150 (400 by 500)	—
R	CO	120 (400)	4 by 24 (12 by 80)	0.57	1.71	2.8 (6.8)	180 by 150 (600 by 500)	Minor damage.

NOTE.—Dash indicates no data available.

MECHANICS OF MASSIVE PILLAR COLLAPSES

A conceptual model of a massive pillar collapse can be described as follows. Undersized, regularly spaced remnant pillars help the stiff and competent roof to bridge a relatively wide span. A pressure arch is created, with much of the overburden load being transferred by the stiff roof to the barrier pillars surrounding the extraction area. Within the pressure arch, the pillars are shielded from the full weight of the overburden. Eventually, any one of a number of mechanisms may cause the pressure arch to break down:

• The extraction area becomes so large that it exceeds the bridging capacity of the roof.
  • Mining approaches a fault or other discontinuity.
  • The roof weakens over time.
  • The remnant pillars weaken over time.

Once the pressure arch breaks down and additional overburden load is shifted to the pillars, their structural characteristics are such that a sudden, massive collapse can occur. Slender pillars have little residual strength and shed load rapidly as they fail. When one fails, the weight it transfers can overload adjacent pillars, and a rapid "domino" failure of adjacent pillars can ensue. Pillars that are more squat retain most of their load even after failure. Such pillars will squeeze slowly, rather than collapse.

Laboratory tests have shown that the residual strength of coal specimens depends on their w/h ratio [Das 1986]. Specimens with a w/h ratio of less than 3 typically have little residual strength, which means that they shed almost their entire load when they fail (figure 4). As the specimens become more squat, their residual strength increases. Once the w/h ratio reaches 8-10, the specimens become "strain-hardening," which means that they never shed load, and sudden collapse is impossible.

Figure 5 summarizes available postfailure modulus data for large in situ coal specimens and full-scale coal pillars. The dashed line indicates a conservative envelope for these limited in situ data. In general, the laboratory postfailure moduli exceed the large-scale test values.

The importance of the postfailure stiffness is further explained by the theory of *local mine stiffness*, first proposed by Salamon [1970] and discussed by Zipf [1992, 1996]. The theory states that if the pillar's postfailure modulus (K_p) is less than the stiffness of the mine roof (the local mine stiffness, or K_M), the failure is stable and gradual (figure 6B). If K_p exceeds K_M, on the other hand, the failure is sudden and violent (figure 6A). The local mine stiffness depends on the modulus of the immediate roof; floor and pillar materials; and the layout of pillars, mine openings, and barrier pillars. The post-failure stiffness, K_p, depends on the w/h ratio of the coal pillar, as shown in figure 5. Using a boundary-element method program similar to the USBM's MULSIM/NL program, it is possible to simulate both massive pillar collapses and stable, progressive pillar failures [Zipf 1996]. The behavior of computer simulations changes depending on whether the model satisfies or violates the local mine stiffness stability criterion.
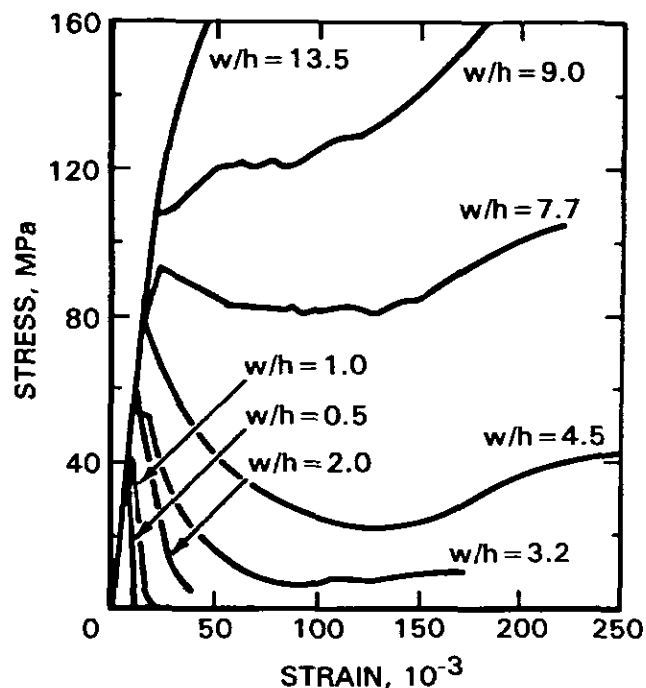

Figure 4.—Complete stress-strain curves for Indian coal specimens, showing increasing residual strength with increasing w/h ratio (after Das [1986]).
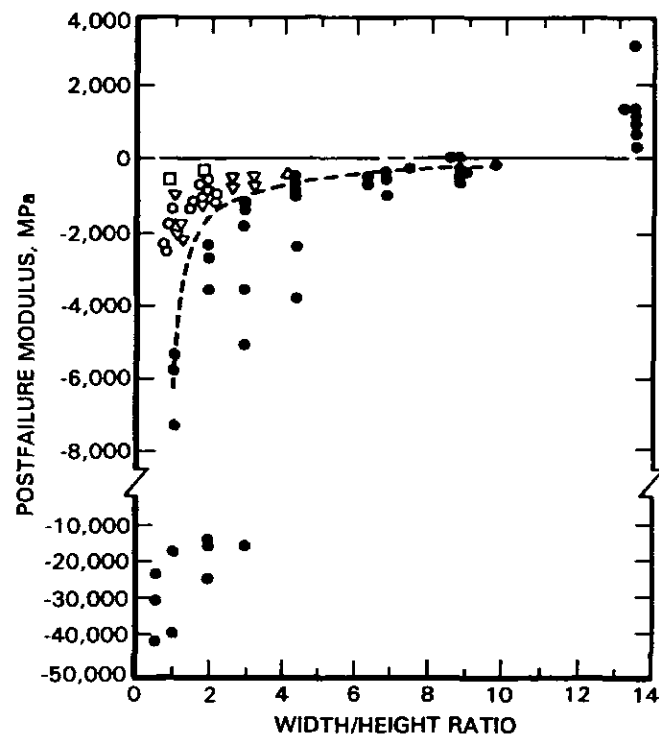

Figure 5.—Postfailure modulus of coal pillars, in situ coal specimens, and laboratory samples. Darkened circles represent laboratory tests, remaining symbols represent in situ tests [Chase et al. 1994].
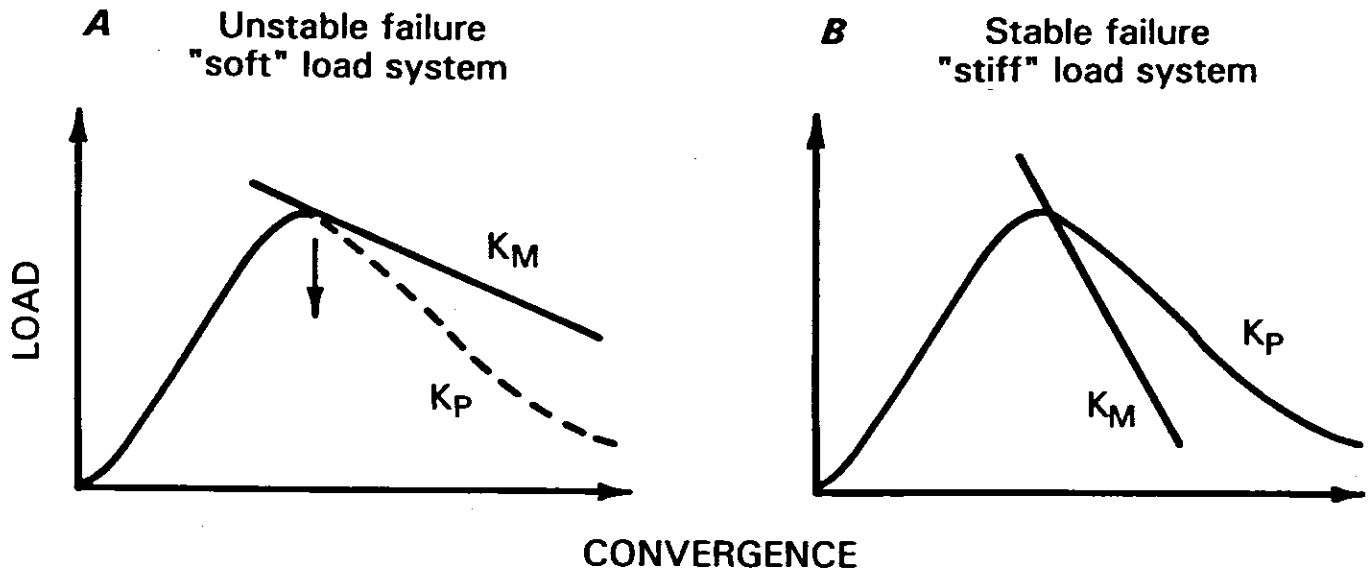
A Unstable failure "soft" load system

B Stable failure "stiff" load system

Figure 6.—Illustration of the local mine stiffness concept. A, local mine stiffness (K_M) is less than postfailure stiffness of the pillar (K_P), resulting in unstable failure. B, local mine stiffness (K_M) exceeds the pillar's postfailure stiffness (K_P), resulting in slow and stable failure.

DESIGN APPROACHES TO CONTROL MASSIVE PILLAR COLLAPSE

In coal mining, small-center mining and partial pillaring are methods to achieve high extraction without full pillar recovery. Both leave significant remnant pillars in the mined-out areas. For example, mining on 15-m (50-ft) centers using 6-m (20-ft) entries leaves about 35% of the coal in 9- by 9-m (30- by 30-ft) pillars. Splitting pillars developed on 18- by 18-m (60- by 60-ft) centers leaves about 22% of the coal. Both techniques can be adapted to avoid massive pillar collapses following the strategies of *prevention* or *containment*.

In the *prevention* approach, the panel pillars are designed so that collapse is highly unlikely. This can be accomplished by increasing either the SF of the pillars or their w/h ratio. In the *containment* approach, high extraction is practiced within individual compartments that are separated by barriers. The small pillars may collapse within a compartment; however, because the compartment size is limited, the consequences are not significant. The barriers may be true barrier pillars, or they may be rows of development pillars that are not split on retreat. The containment approach has been likened to the use of compartments on a submarine.

Full extraction can be another strategy to avoid massive pillar collapses. Mining all of the coal removes the support to

the main roof, thereby limiting the potential width of the pressure arch. Although some "first falls" behind longwalls and other full-extraction systems have been destructive, they generally involve areas smaller than massive pillar collapses.

SMALL-CENTER MINING: A PREVENTION APPROACH

Square pillars are generally used in small-center mining. Table 1 indicates that three collapses involved 9-m (30-ft) square pillars, and one involved 12-m (40-ft) square pillars. Square pillars may be designed to be collapse-resistant in two ways. The first is to increase their w/h ratio. Because no collapses have been documented in which the w/h ratio was greater than 3.0, a design w/h ratio of 4.0 is suggested to provide an adequate margin of safety.

Pillar collapses may also be avoided by maintaining a sufficiently high SF. The ARMPS case history data base [Mark and Chase 1997] suggests that normally an ARMPS SF of 1.5 is sufficient to limit the probability of pillar failure. Where slender pillars are being employed and their failure may result in a massive collapse rather than a slow squeeze, it
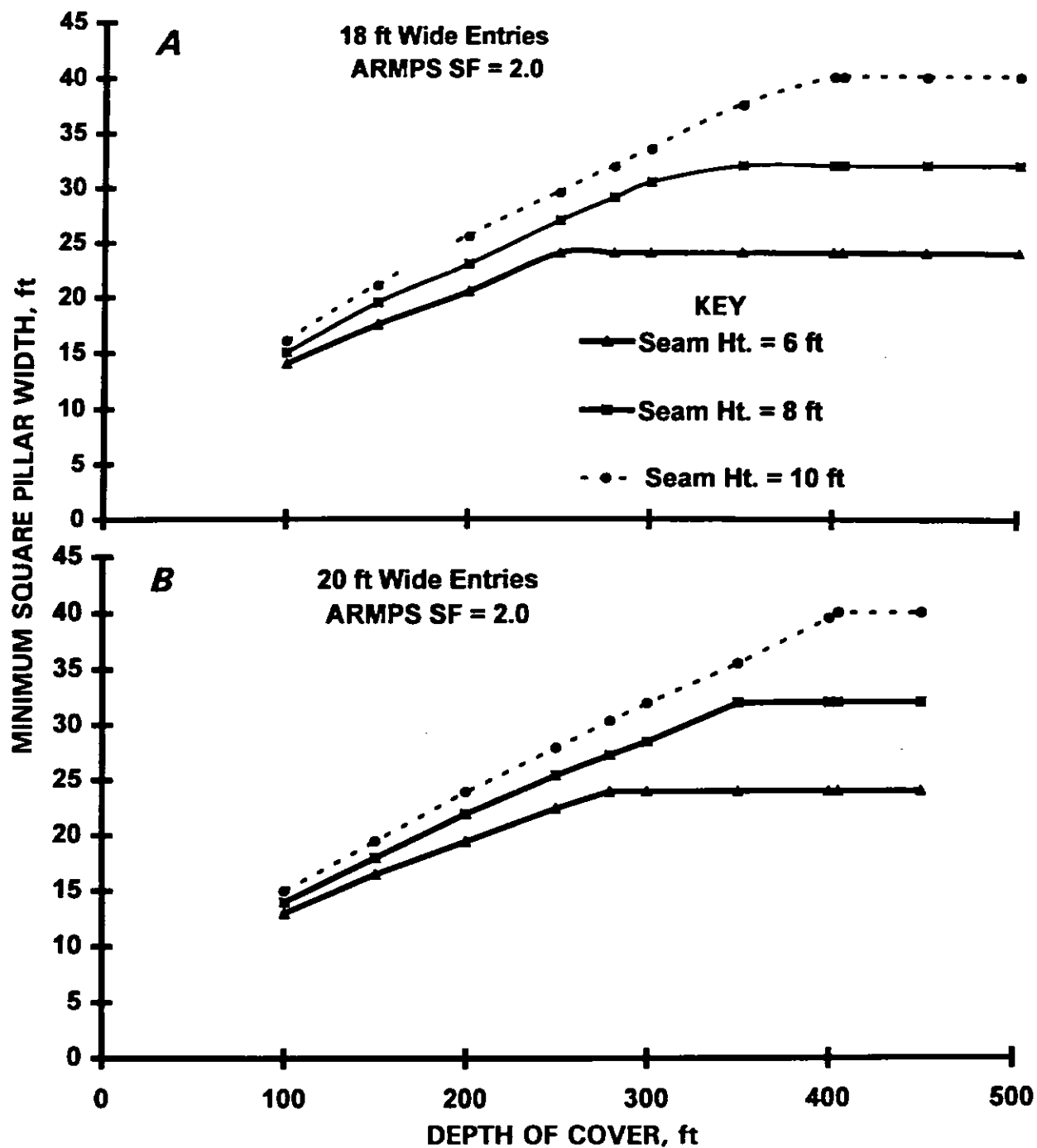
Figure 7.—Suggested minimum square pillar size to avoid massive pillar collapse. *A*, 5.5-m (18-ft) entries; *B*, 6-m (20-ft) entries.

might be prudent to increase the SF to 2.0. The SF can be increased by increasing the pillar width, decreasing the extraction ratio, or both. These two design criteria have been combined to develop guidelines for small-center mining. Figure 7 was developed assuming square pillars with an SF of 2.0 or a w/h ratio of 4.0.

When using 6-m (20-ft) wide entries, the minimum suggested pillar sizes are increased by about 6%. Also note that these design criteria are only for controlling massive pillar collapses. At greater depths, pillar sizes may need to be increased beyond a w/h ratio of 4 to maintain an adequate SF. The failure of pillars with a w/h ratio greater than 4 should be a slow squeeze rather than a sudden collapse.

PILLAR SPLITTING: A CONTAINMENT APPROACH

Fenders left from pillar-splitting operations have failed at even shallow depths. For example, 3- by 12-m (10- by 40-ft) fenders in a 3-m (10-ft) seam have an SF of 1.5 at only 55 m (180 ft) of cover. The potential for a destructive massive collapse can be reduced by limiting the size of the gob area. To separate the gob areas, rows of unsplit development pillars can be left as barriers. This strategy is based on two assumptions:

- By limiting the span above the mined-out area, a bridging failure of the strong overburden is less likely.
- By minimizing the size of the potential collapsed area, any airblast resulting from a collapse would be less powerful.

Table 1 shows that no major collapses have been documented in which the gob area was less than 1.5 ha (4 acres). In the five cases where the gob area was between 1.5 and 1.9 ha (4 and 5 acres), about 60% of the incidents resulted in major damage. Additionally, no damaging incidents occurred when the minimum dimension of the mined-out area was less than 100 m (350 ft). Using these data, acceptable dimensions of a pillar-splitting operation might be a maximum area of 1.2 ha (3.2 acres), with a minimum dimension of less than 90 m (300 ft). For example:

- Assuming 18- by 18-m (60- by 60-ft) centers in a nine-entry system with four rows split, the mined-out area would

have a minimum dimension of 72 m (240 ft) and an area of about 1.1 ha (3 acres), as shown in figures 8A and 8B.

- Assuming the same pillar size in a six-entry system with five rows split, the minimum dimension would be 90 m (300 ft) and the area would be about 1 ha (2.5 acres), as shown in figures 8C and 8D.

The next question is: how many unsplit rows should be left between these mined-out areas? The goal is to leave enough of a "barrier" so that the failure of one gob area does not initiate failure in adjacent areas. ARMPS was used to evaluate the loading on unsplit pillars between two mined-out areas. The program was modified so that two "front" gobs could be applied to the unsplit pillars. The analyses were run with abutment angles of 90°, which assumes that none of the load is carried by the gob, but instead is transferred to the barriers.

In the first set of analyses, two rows of full-sized pillars were used as the barrier. An ARMPS SF of 1.5 was deemed necessary to prevent the collapse of one gob area triggering the collapse of an adjacent area. Three rows of pillars were used in the second set of analyses; the SF was reduced to 1.0 because of the greater stiffness of the barrier. Pillars on 18- by 18-m (60- by 60-ft) centers were used in all cases.

Other parameters that were varied included the number of rows that were split (three, four, and five), the entry width (5.5 and 6 m (18 and 20 ft)), the seam height (2, 2.5, and 3 m (6, 8, and 10 ft)), and the number of entries in the section (five, seven, and nine). The results are presented in figure 9, which shows the suggested maximum depth of cover for each combination of parameters. In general, considering 5.5-m (18-ft) entries in a 2.5-m (8-ft) seam, it appears that two rows of unsplit pillars are an adequate barrier at depths less than about 300 ft and that three rows are acceptable to about 170 m (550 ft) of cover.

Barriers must also be left between extracted panels. These can be unsplit development pillars or solid coal. If unsplit development pillars are used, the analysis in figure 9 should apply. For solid coal barriers, figure 10 shows the suggested widths, using the same loading assumptions. For a 2.5-m (8-ft) seam, a 17-m (55-ft) solid barrier appears to be appropriate at 75 m (250 ft) of cover, and 23 m (75 ft) might be needed at 120 m (400 ft).
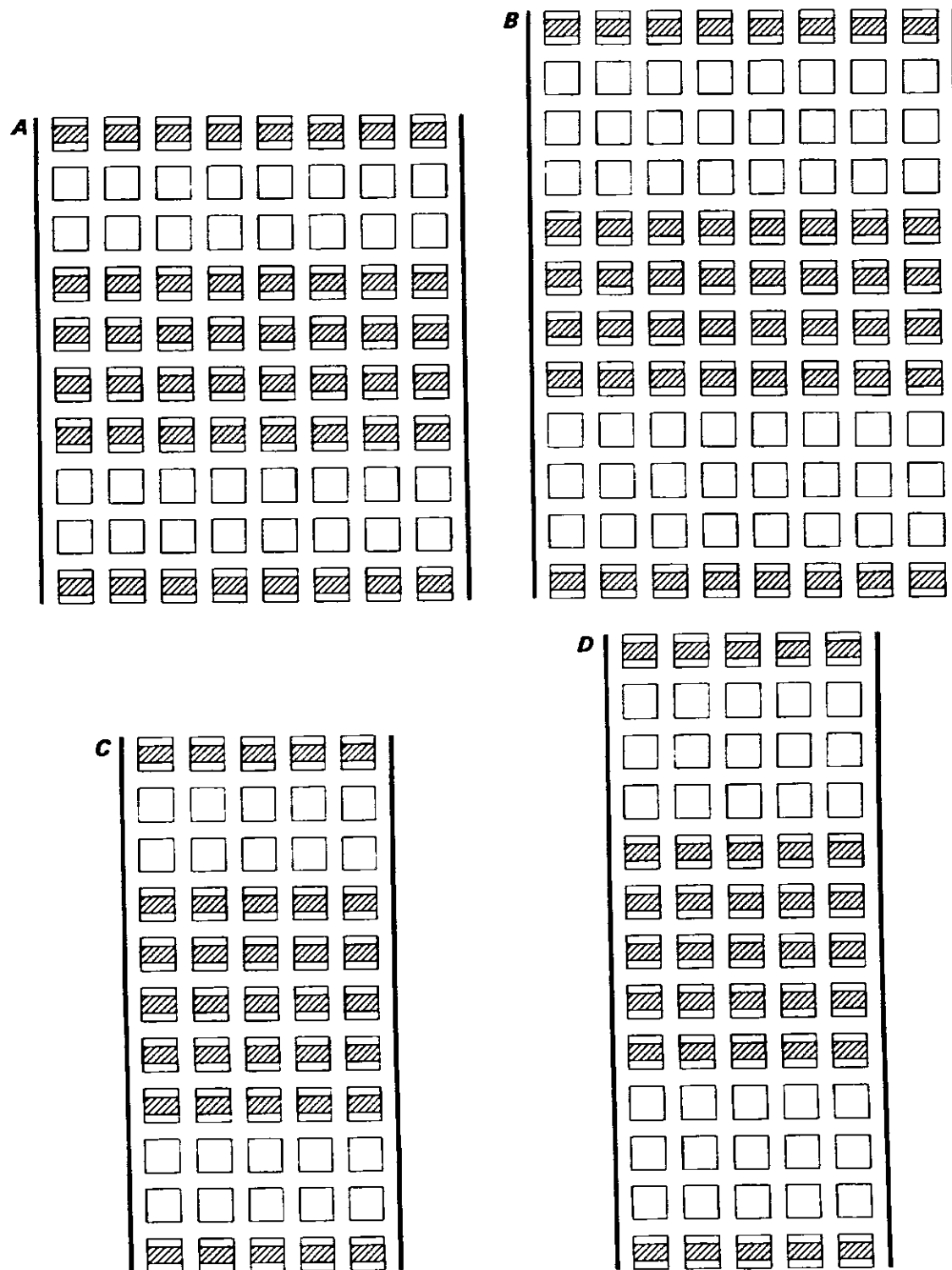
Figure 8.—Possible pillar-splitting plan for airblast control. *A*, nine-entry system, two rows of unsplit pillars for barrier. *B*, nine-entry system, three rows of unsplit pillars for barrier. *C*, six-entry system, two rows of unsplit pillars for barrier. *D*, six-entry system, three rows of unsplit pillars for barrier.
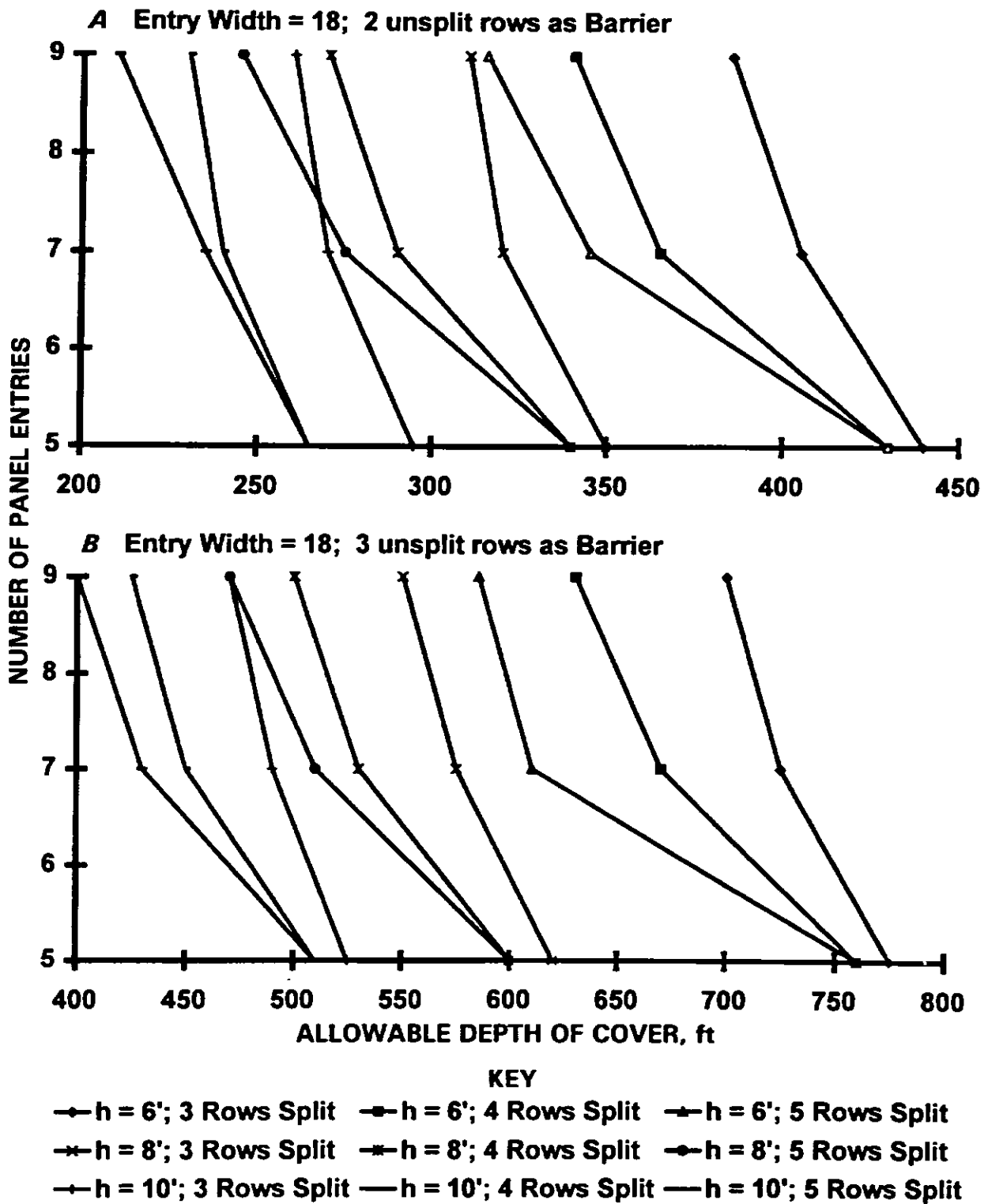
Figure 9.—A, suggested maximum depth for two rows of unsplit pillars as barrier between gob areas, 5.5-m (18-ft) entry, 18-by 18-m (60- by 60-ft) pillars. B, suggested maximum depth for three rows of unsplit pillars as barrier between gob areas, same entry and pillar sizes.
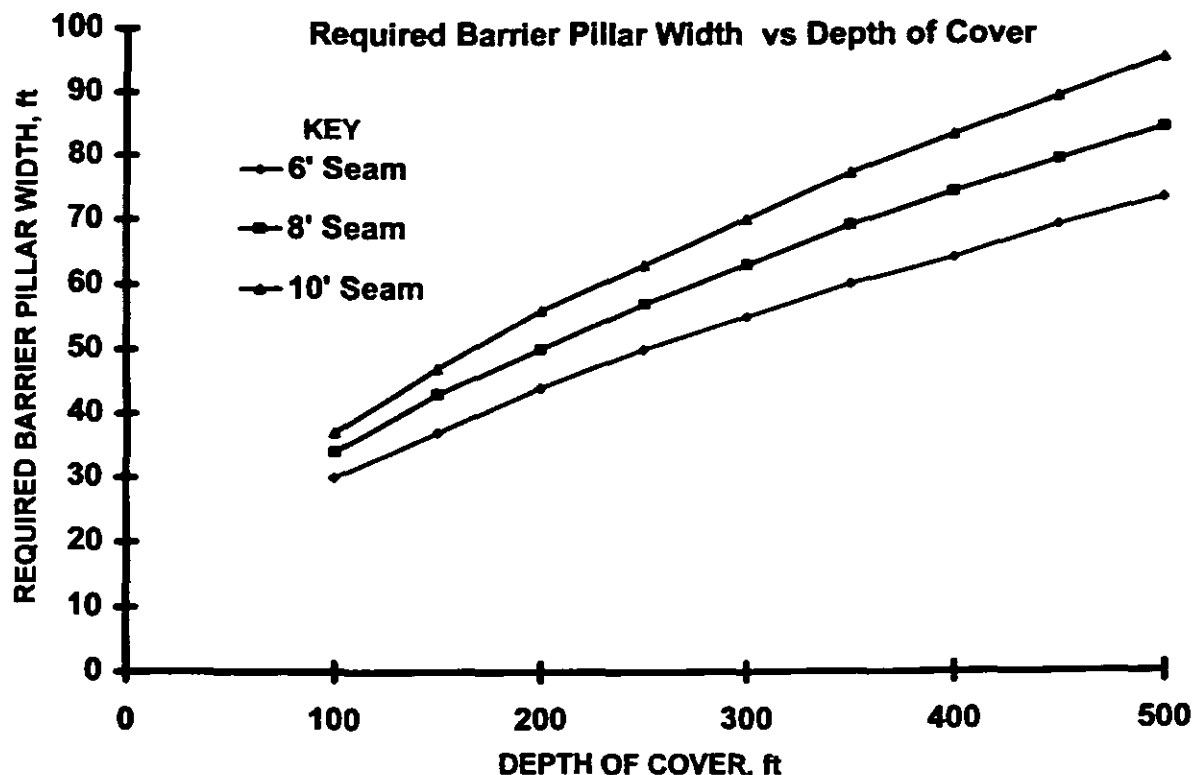
Required Barrier Pillar Width vs Depth of Cover

Figure 10.—Suggested solid coal barrier width between two areas where pillars have been split.

CONCLUSIONS

The potential for massive pillar collapses should always be considered when designing room-and-pillar mining operations. A collapse can occur when one pillar fails suddenly, overstresses its neighbors, causing them to fail, and so forth, in very rapid succession. Very large mining areas can collapse via this mechanism within seconds with little or no warning. The collapse itself can pose serious danger to nearby mining personnel. Additionally, the collapse can induce a violent airblast that disrupts or destroys the ventilation system. Further critical danger to miners exists if the mine atmosphere becomes explosive or contaminated as a result of the pillar collapse.

Research has found that massive collapses in coal mines have the following common characteristics:

• Slender pillars (w/h ratio less than 3.0).
• Low SF (less than 1.5).
• Competent roof strata.
• Collapsed area greater than 1.6 ha (4 acres).
• Minimum dimension of the collapsed areas greater than 110 m (350 ft).

Two alternative strategies may be successful in preventing massive pillar collapses. For small-center mining, *prevention* may be applied by increasing either the w/h ratio or the SF. *Containment* is appropriate for pillar splitting and requires leaving barriers or rows of unsplit pillars to limit the area of potential collapses. A final strategy is to go to full pillar extraction. By removing the support provided by the remnant fenders left during traditional pillar splitting, the bridging capacity of the roof should be substantially reduced.

Finally, it is important to note that the massive pillar collapses discussed in this paper are not to be confused with coal bumps or rock bursts. Although the outcomes may appear similar, the underlying mechanics are entirely different. Bumps are sudden, violent failures that occur near coal mine entries and expel large amounts of coal and rock into the excavation [Maleki 1995]. They occur at great depth, affect pillars (and longwall panels) with large w/h ratios, and are often associated with mining-induced seismicity. The design recommendations discussed here for massive pillar collapses do *not* apply to coal bump control.

REFERENCES

Bryan A, Bryan JG, Fouche J [1966]. Some problems of strata control and support in pillar workings. Min Eng (London) *123*:238-254.

Chase FE, Zipf RK, Mark C [1994]. The massive collapse of coal pillars - case histories from the United States. In: Proceedings of the 13th Conference on Ground Control in Mining. Morgantown, WV: West Virginia University, pp. 69-80.

Das MN [1986]. Influence of width/height ratio on postfailure behavior of coal. Intl J Min Geol Eng *4*:79-87.

Ferriter RL, Zipf RK, Ropchan DM, Davidson J [1996]. Report of technical investigation underground nonmetal mine collapse accident, Solvay Mine. U.S. Department of Labor, Mine Safety and Health Administration.

Madden BJ [1991]. A re-assessment of coal pillar design. J South Afr Inst Min Metall *91*(1):27-37.

Maleki H [1995]. An analysis of violent failure in U.S. coal mines—case studies. In: Maleki H, Wopat PF, Repsher RC, Tuchman RJ, eds. Proceedings: Mechanics and Mitigation of Violent Failure in Coal and Hard-Rock Mines. Pittsburgh, PA: U.S. Department of the Interior, Bureau of Mines, SP 01-95, pp. 5-25.

Mark C, Chase FE [1997]. Analysis of retreat mining pillar stability (ARMPS). In: Mark C, Tuchman RJ, comp. Proceedings: New Technology for Ground Control in Retreat Mining. Pittsburgh, PA: U.S. Department of Health

and Human Services, Public Health Service, Centers for Disease Control, National Institute for Occupational Safety and Health, IC 9446.

Ropchan D [1991]. Ground support evaluation—Belina No. 2 Mine ID No. 42-01280. Denver, CO: U.S. Department of Labor, Mine Safety and Health Administration.

Salamon MDG [1970]. Stability, instability, and design of pillar workings. Intl J Rock Mech Min Sci *7*:613-631.

University of New South Wales School of Mines [1994]. Pillar performance. Strata Control for Coal Mine Design *Apr:5*.

Zipf RK Jr. [1992]. Analysis of stable and unstable pillar failure using a local mine stiffness method. In: Iannacchione AT, Mark C, Repsher RC, Tuchman RJ, Jones CC, comp. Proceedings of the Workshop on Coal Pillar Mechanics and Design. Pittsburgh, PA: U.S. Department of the Interior, Bureau of Mines, IC 9315, pp. 128-143.

Zipf RK [1996]. Analysis and design methods to control cascading pillar failure in room-and-pillar mines. In: Bieniawski ZT, ed. Milestones in Rock Engineering, Balkema, pp. 225-264.

Zipf RK, Mark C [1996]. Design methods to control violent pillar failures in room-and-pillar mines. In: Proceedings of the 15th Conference on Ground Control in Mining. Golden, CO: Colorado School of Mines, pp. 571-585.